博士論文番号：**1481204**
(Doctoral student number)

Functional Elucidation of MTMR3 and MTMR4 in Innate Immune Response

自然免疫応答における **MTMR3** と **MTMR4** の機能的役割の解明

Dyaningtyas Dewi Pamungkas Putri

Nara Institute Science and Technology
Graduated School of Biological Sciences and Technology
Immunobiology Molecular
Supervisor Prof. Taro Kawai
(September 14, 2018)

List of Figure

List of Table

Abbreviations

PAMPs	Pathogen-Associated Molecular Patterns
PRRs	Pattern-Recognition Receptor
IFNs	Interferons
TLRs	Toll-Like Receptors
RLRs	Retinoic acid-inducible gene I-Like Receptors
RIG-I	Retinoic acid-inducible gene-I
MDA-5	Melanoma differentiated gene 5
cGAS	Cyclic GMP-AMP synthase
cGAMP	Cyclic guanosine monophosphate–adenosine monophosphate
ISD	Interferon Stimulatory DNA
LPS	Lipopolysaccharide
Poly I:C	Polyinosinic:polycytidylic acid
MyD88	Myeloid differentiation factor 88
TRIF	TIR-domain-containing adapter-inducing interferon-β
dsRNA	Double-stranded RNA
IPS-1	Interferon-β promoter stimulator 1
CARD	Caspase Activation and Recruitment Domain
STING	Stimulator of interferon genes
TBK1	TANK-binding kinase 1
IRF3	Interferon Regulatory Factor-3
NF-κB	Nuclear Factor k-light-chain-enhancer of activated B cells
ER	Endoplasmic reticulum
TRAP	Translocon-associated protein
SSR2	Translocon-associated protein (TRAP) complex TRAPβ
iRhom2	inactive Rhomboid protein 2
BafA1	Bafilomycin A1
PtdIns	Phosphatidylinositol
PtdIns3P	Phosphatidylinositol 3-phosphate
PtdIns5P	Phosphatidylinositol 5-phosphate
MTMs	Myotubularins
MTMR3	Myotubularin-related phosphatase 3

MTMR4	Myotubularin-related phosphatase 4
HEK	Human embryonic kidney
DMEM	Dulbecco's Modified Eagle's Medium
HRP	Horseradish peroxidase
SDS PAGE	Sodium dodecyl sulfate polyacrylamide gel electrophoresis
KO	Knockout
DKO	Double Knockout
TracrRNA	Trans activating CRISPR RNA

1. Introduction

1.1 Innate immunity

Host immune response is a defense system to eliminate to invading pathogens including bacteria, fungi, and virus, and largely classified into innate and acquired immune responses. Innate immune response is the first line of host defense system that is triggered upon sensing molecules specific in pathogens, which are called Pathogen-Associated Molecular Patterns (PAMPs) with Pattern-Recognition Receptor (PRRs) that are expressed in various types of host cells such as macrophages, dendritic cells, endothelial cells, epithelial cells and lymphocytes (Kawai et al., 2010; Iwasaki et al., 2015). Among them, dendritic cells and macrophages are the major innate immune cells that produce large amounts of pro-inflammatory cytokines and type I interferons (IFNs) and function as antigen presenting cells that potentiate acquired immunity. Releasing cytokines and type I IFNs lead to production of anti-bacterial or anti-viral proteins to prevent pathogen infections. In addition, cytokine production and antigen presentation by innate immune cells induce acquired immune activation, which includes antibody production by plasma cells and T cell-specific killer activity.

So far, numerous PRRs have been identified. These include Toll-Like Receptors (TLRs), Retinoic acid-inducible gene I (RIG-I)-Like Receptor (RLRs), and intracellular sensor for DNA such as cyclic GMP-AMP synthase (cGAS). They recognize different or overlapped PAMPs at different organelles such as the transmembrane, endosomes, nucleus or cytoplasm, and activate distinct signaling pathways. These differences result in appropriate immune responses specific to given pathogens (Kawai et al., 2011).

1.2 PRRs and their signaling pathways

TLRs are comprised of about 10 members in mammals and consist of extracellular leucine-rich repeats and cytoplasmic Toll/interleukin-1-receptor (TIR) domain. TLR4 recognizes bacterial lipopolysaccharide (Alexander and Rietschel, 2001; Bell, 2008). TLR2 and TLR5 recognize other bacterial components such as peptidoglycan and flagellin, respectively. Unlike these TLRs expressed on the cell surface, TLR3, TLR7 and TLR9 are exclusively expressed in the endosomes and recognize viral or bacterial nucleic acids such as double-stranded RNA (dsRNA), single-stranded RNA (ssRNA) or CpG DNA, respectively (Irving and William, 2009; Broz and Monack, 2013; Pandey et al., 2014). All these TLRs initiate signaling pathways upon PAMPs recognition by recruiting a TIR domain-containing adapter proteins

such as MyD88, TIRAP, TRIF and/or TRAM, and activate the transcription factors such as NF-κB or IRF family members such as IRF3 and IRF7 to induce the transcription of target genes including inflammatory cytokines (IL6, TNF, etc) and type I IFNs (Kagan et al., 2008; Kawai and Akira, 2010).

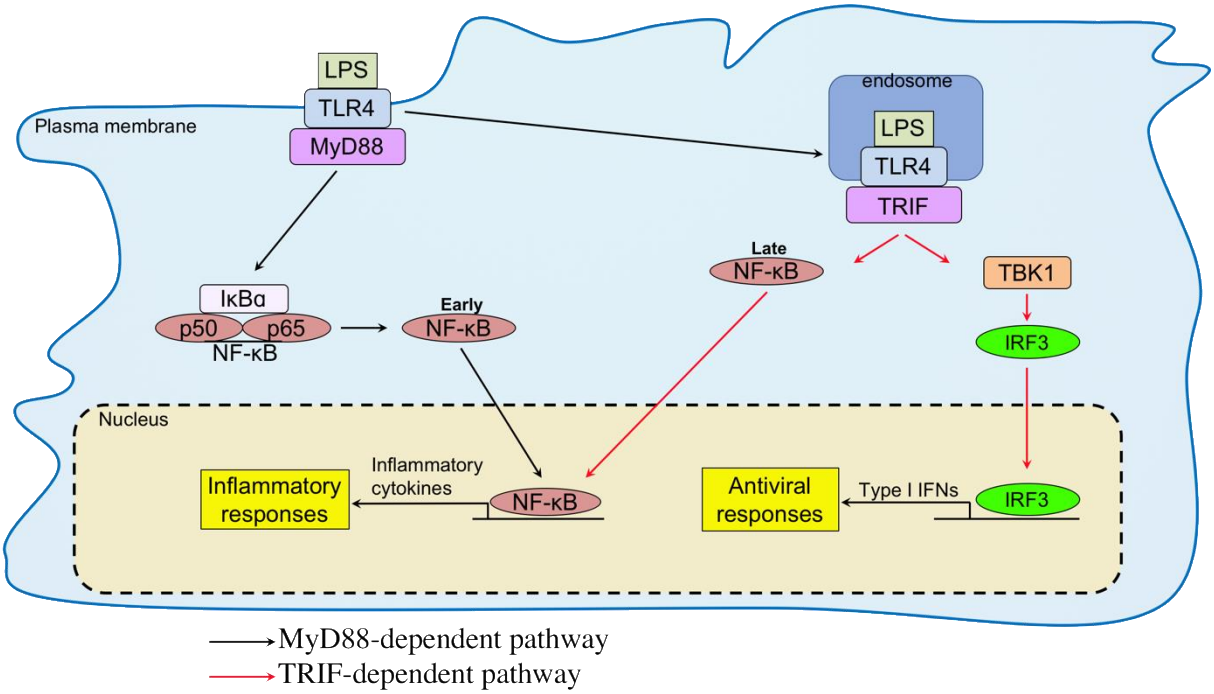

Fig. 1. TLR4 signaling pathway. TLR4 recognizes LPS and activates TIRAP-MyD88 and TRAM-TRIF signaling pathway. TIRAP-MyD88 activates NF-κB at early phase to produce inflammatory cytokines. TLR4 is then trafficked to endosome to activate TRAM-TRIF pathway, which leads to late phase activation of NF-κB and IRF3 to produce inflammatory cytokines and type I IFNs.

RLRs are a family of DExD/H box RNA helicases that recognize viral RNA in the cytoplasm. RLRs consist of RIG-I and MDA5, which share structure similarities such as an N terminal region consisting of tandem caspase activation and recruitment domain (CARD), a central DExD/H box RNA helicase domain responsible for viral RNA recognition and C-terminal domain (CTD) that is involved in autoregulation in the case of RIG-I (Loo and Gale, 2011). In an active state, the CARD domain of RIG-I binds to its central helicase domain. After binding to viral RNA, cytosolic RIG-I and MDA5 undergo conformational changes and associate with the CARD domain of IPS-1, an adapter molecule localized at the mitochondrial outer membrane. IPS-1 subsequently activates IRF3 and NF-κB by recruiting their upstream protein kinases such as TBK1 and IKKα/β, respectively (Kawai et al., 2005; Seth et al., 2005).

RIG-I recognizes 5′-triphosphate RNA (5′-ppRNA) as well as short dsRNA derived from Sendai virus and Newcastle disease virus of Paramyxoviridae virus family, influenza A

virus of the Orthomyxoviridae virus family, Japanese encephalitis virus of Flaviviridae family, vesicular stomatitis virus of the Rhabdovirus family whereas MDA5 recognizes long dsRNA derived from poliovirus of the Picornaviridae family and encephalomyocarditis virus (Pandey, 2014). RLRs are expressed in various cells including immune and non-immune cells, which are in contrast to nucleic acids-recognizing TLRs that are abundantly expressed on innate immune cells such as macrophages and dendritic cells. Thus, RLRs are cytoplasmic sensors for RNA viruses that are infected into cells whereas TLRs recognize viruses that are engulfed and lysed in the endosomes by innate immune cells.

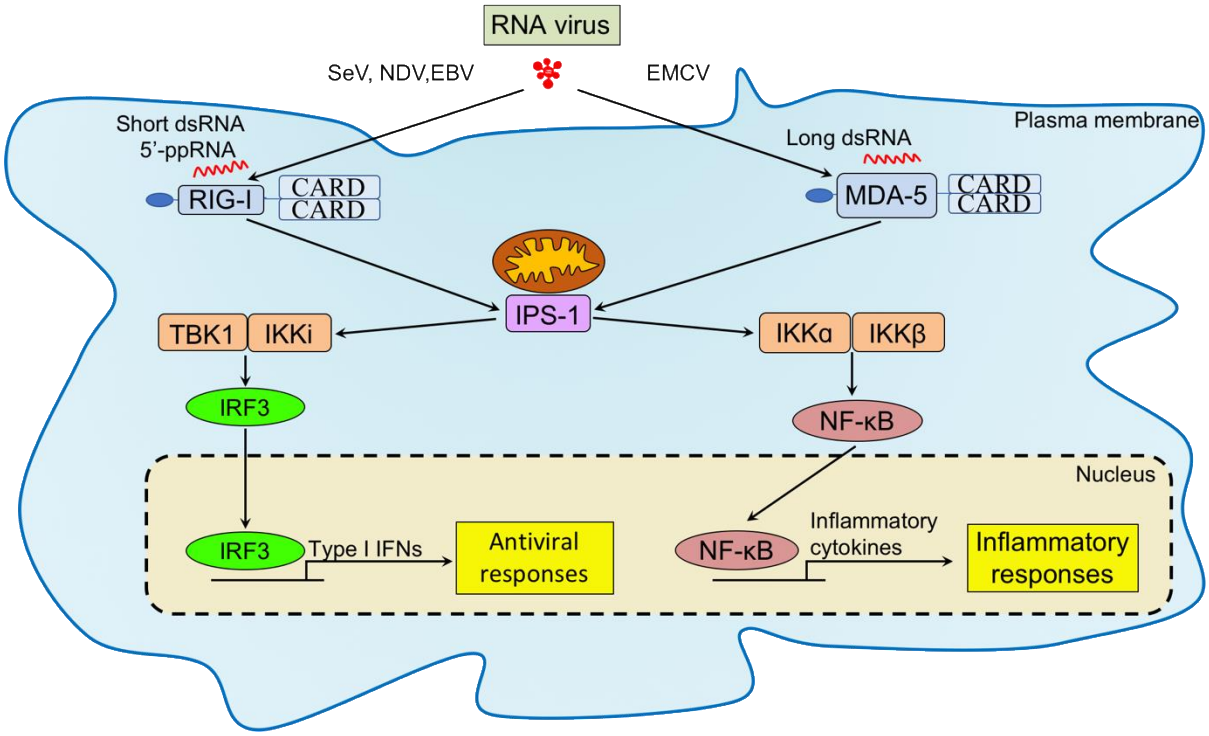

Fig. 2. RLR signaling pathway. Short dsRNA and long dsRNA are recognized by RIG-I and MDA5, respectively. RIG-I and MDA5 bind to an adapter IPS-1 to active TBK1-IRF3 and IKKα/β-NF-κB and induce type I IFN and inflammatory cytokines.

Host cells also express a cytosolic sensor responsible for DNA recognition. cGAS are identified as a cytoplasmic DNA sensor. cGAS is an enzyme that synthesizes cGAMP from ATP and GTP following binding to viral and host DNA. cGAMP contains two phosphodiester bonds, one between 2′-OH of GMP and 5′-phosphate of AMP and the others between 3′-OH of AMP and 5′-phosphatase of GMP (Zhang et al., 2013) and acts as the second messenger that binds to the adaptor protein STING on endoplasmic reticulum (ER). STING traffics from the ER to perinuclear region including the Golgi apparatus, then forms punctate structures along with TBK1. TBK1 phosphorylates IRF3 and phosphorylated IRF3 forms a dimer and

translocate into nucleus to express type I IFN genes. Therefore, translocation of STING to Golgi is a hallmark of activation of STING. Various types of DNA viruses such as human papillomavirus, herpes simplex virus, adenovirus, hepatitis B virus infect to the host cells and release their own DNA genome to cytoplasm of host cells. cGAS in host cells binds to the released viral DNA and cGAS recognition initiates innate immune responses. cGAS also recognizes retroviruses such as HIV-1, which produces intermediate DNA from viral RNA genome during expansion (Ma and Damania, 2016). Also, cGAS binds to host cell DNA when cells are damaged by environmental stresses, aging, and drug, and this response contributes to autoimmunity and inflammation as well as potentiation of acquired immune responses to cancers (Lau et al., 2015; Mackenzie et al., 2017; Wang et al., 2017; Yang et al., 2017, Xiong et al 2018).

1.3 Regulatory mechanisms of cGAS-STING signaling pathways

Various regulatory mechanisms for cGAS and STING pathway have been shown (Cai et al., 2014; Chen and Chen, 2016; Liu et at., 2015; Liu and Wang 2016; Hu et al., 2016). Sumoylation and Mono-ubiquitination of cGAS at Lys355 that are induced by E3 ubiquitin ligase TRIM56 is important for its DNA sensing activity, resulting in increased cGAMP production (Xiong et al., 2018; Sun et al., 2013; Seo et al., 2018). STING moves from ER to Golgi apparatus via the translocon-associated protein (TRAP) complex TRAPβ (SSR2) that is recruited by inactive rhomboid protein 2 (iRhom2) and these complex reaches to Sec-5 containing perinuclear microsome or cytoplasmic punctate structures to assemble with TBK1 and IKK complex (Ishikawa et al., 2008; Abe and Barber, 2014; Luo et al, 2016). RAB2B-GARIL5 (Golgi-associated RAB2B interactor-like 5) complex is a regulator of STING in Golgi apparatus and promotes IFN response through regulating phosphorylation of IRF3 by TBK1. The autophagy-related protein such as autophagy-related protein (Atg), ULK1 (a homologue of Atg1), microtubule-associated protein 1 light chain (LC)3 (homologue of yeast Atg8) and Atg9 negatively regulate STING signaling through interfering with STING-TBK1-IRF3 signaling (Saitoh et al., 2009, Tooze et al., 2010; Konno et al., 2013). Atg-mediated degradation modulates baseline of STING protein level, but it does not impact the trafficking of STING. The function of STING is regulated by post-translational mechanism such as TRIM32 and TRIM56, that conjugate K63-linked polyubiquitination on STING and promote the recruitment of TBK1 (Tsuchida et al., 2010). ER-associated E3 ligase, AMFR, catalyzes the K27-linked polyubiquitination of STING together with INSIG1 (Wang et al., 2014). K27-linked

polyubiquitination on STING induces TBK1 recruitment and activation. iRhom2, which recruits de-ubiquitination enzyme EIF3S, maintains the stability STING through removal of its K48-linked polyubiquitin chains. STING translocates from ER to Golgi apparatus and then moves to late endosome/lysosome (Dobbs et al., 2015). Helix aa281-297 of STING is shown to be degraded through V-ATPase in endosome/lysosome. The blockade of V-ATPase suppresses STING degradation, which potentially leads to enhance STING signaling (Gonugunta et al., 2017).

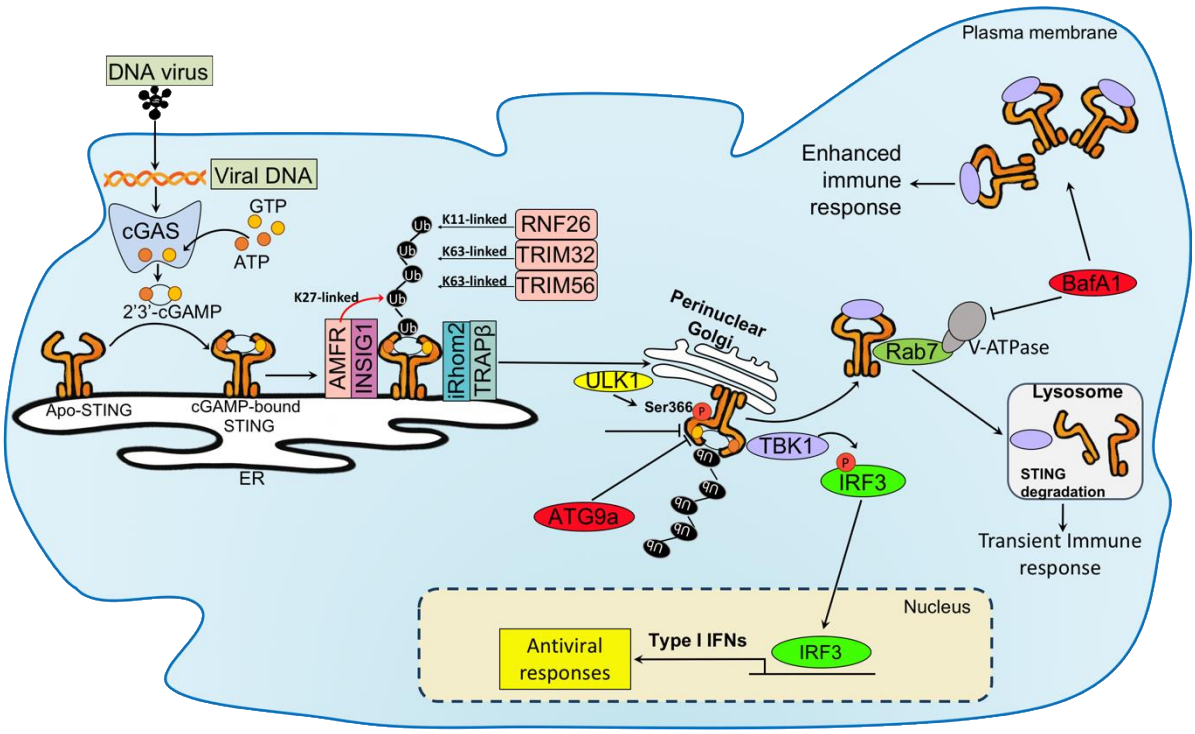

Fig. 3. STING-mediated DNA sensing signaling pathway. cGAS binds to DNA and synthesizes cGAMP which activates STING. AMFR-INSIG1 catalyzes K27-linked ubiquitination on STING and activates TBK1. iRhom2 and TRAPβ mediate the trafficking of STING to Golgi. RNF26, TRIM32, and TRIM56 modulate ubiquitination on STING. ATG9a controls the translocation of STING. V-ATPase regulates Rab7-mediated translocation of STING to lysosome and degradation of STING. Inhibition of V-ATPase by BafA1 suppresses STING degradation and enhances innate immune response.

1.4 Phosphatidylinositol in immune system

Phosphatidylinositol (PtdIns) consists of inositol ring and acyl chains which are linked by phosphate. Inositol ring in PtdIns has three phosphorylation sites (3′, 4′ and 5′) which are phosphorylated by different combinations. Therefore, PtdIns has 8 types; PtdIns, PtdIns3P, PtdIns4P, PtdIns5P, PtdIns(3,4)P_2, PtdIns(3,5)P_2, PtdIns(4,5)P_2, PtdIns(3,4,5)P_3, which regulate distinct cellular processes and protein regulatory functions such as membrane trafficking, signal transduction and immune responses (Wymann and Schneiter, 2008). These PtdIns are phosphorylated and dephosphorylated at the specific sites in inositol ring by various types of polyphosphoinositide kinases and phosphatase. Among them, several kinases and

phosphatases are reported to be contributing to the regulation of immune response. PI5P4Kγ converts PtdIns5P to PtdIns(4,5)P_2 and plays a role in the regulation of the immune system via mTOR pathway (Shim et al., 2016). p110, an isoform of Phosphoinositide 3 kinase, functions as a modulator of leukocyte response (Costa et al., 2011; Costa et al., 2015). TIRAP, a TIR domain-containing adapter protein recruited to TLR4, contains PtdIns(4,5)P_2 binding domain which mediates TIRAP recruitment into plasma membrane to activate NF-κB pathway (Kagan et al., 2008). It has been previously shown that PIKfyve, kinase which phosphorylates 5′ site in inositol ring, produces PtdIns5P, which induces antiviral innate immune response by activating TBK-1-IRF3 axis during RNA virus infection (Kawasaki et al., 2013).

1.5 Myotubularin family

The myotubularins (MTMs) are members of the protein phosphatase superfamily that consists of 1 MTM and 13 MTM-related (MTMR) members and are divided into six subgroups. Among them, three subgroups of MTMs have the catalytically active site of phosphatase consensus site; catalytic Cys–x5-Arg (Cx5R) motif (Table 1). Whereas other three subgroups encompass an inactive catalytic active domain with a lack of cysteine in the phosphatase domain. MTMs are phosphoinositide 3-phosphatase that dephosphorylate 3 positions on inositol, and convert PtdIns3P to PtdIns and PtdIns(3,5)P_2 to PtdIns5P (Fig. 4). Biochemical analysis showed that PtdIns3P works as the substrate for MTM1 and MTMR3, and PtdIns(3,5)P_2 is the substrate for MTMR3 (Clague and Lorenzo, 2005, Tronchère et al., 2012). MTMs have regulatory roles for cellular homeostasis such as immunity, cellular regulation, and membrane trafficking. Previous study reported that MTMR6 negatively regulates Ca^{2+}-activated K channel, K_{ca}3.1 through decreasing PtdIns3P level and the K_{ca}3.1 regulation by MTMR6 is essential for controlling T cell proliferation (Srivastava et al, 2005; Hnia et al., 2012). Active complex formation between MTMR9 and MTMR8 reduced cellular PtdIns3P level and inhibited autophagy process (Zou et al., 2012).

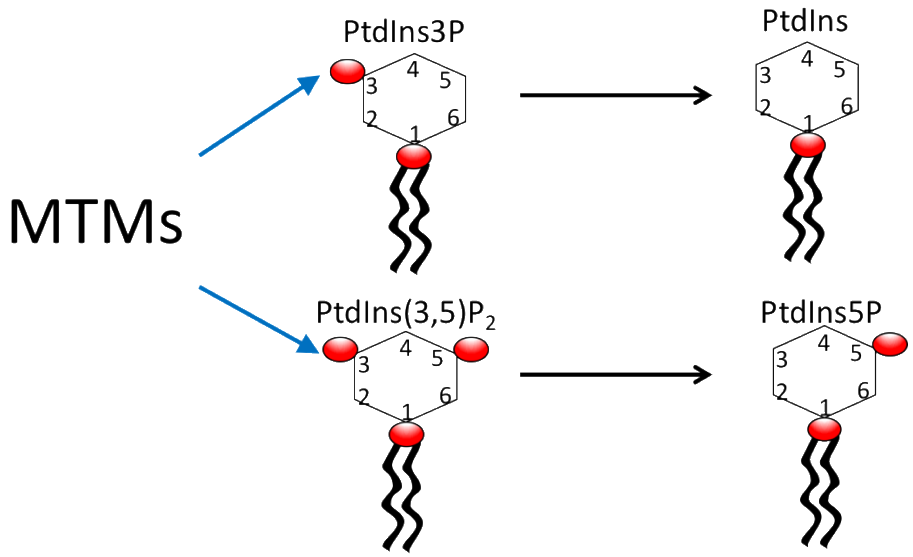

Fig. 4. MTM family members dephosphorylate 3 positions on inositol. MTMs dephosphorylate PtdIns3P to generate PtdIns and dephosphorylate PtdIns (3,5) P_2 to generate PtdIns5P

Table 1. Domain structure for Myotubularin family

Myotubularin (MTMR) family			
MTM1 Subgroup	MTM1	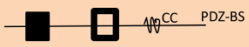	
	MTMR1		
	MTMR2		
MTMR3 Subgroup	MTMR3		Contribute to intestinal inflammation by enhancing cytokine secretion and caspase-1 activation
	MTMR4		
MTMR6 Subgroup	MTMR6		
	MTMR7		
	MTMR8		
MTMR5 Subgroup	MTMR5	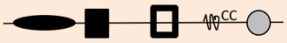	
	MTMR10		
MTMR 9 Subgroup	MTMR9		
MTMR10 Subgroup	MTMR10	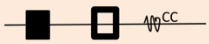	
	MTMR11		
	MTMR12		
DENN PH-G PTP/DSP Coiled-coil Fyve PI3P PH PIP2, PIP3			

1.6 MTMR3 and MTMR4

MTMR3 and MTMR4 are closely related members among MTMRs. MTMR3 and MTMR4 have the phosphatase activity and have the FYVE domain that can potentially bind to PtdIns3P. These MTMRs are reported to form a heteromeric interaction, which increases their enzyme activities and alters their subcellular distribution patterns (Denis et al., 2015). MTMR3 localizes in the cytoplasm and the endosomal membrane, and MTMR4 localizes in the

cytoplasm, early and recycling endosomes (Clague and Lorenzo, 2005; Lorenzo et al., 2005; Naughtin et al., 2010). MTMR3 and MTMR4 are reported to have various cellular functions by producing PtdIns5P. PtdIns5P produced from MTMR3 regulates cellular migration through Rho GTPase RAC1 (Oppelt et al., 2014). MTMR4 regulates transport of a transferrin receptor from early endosome and cellular distribution of recycling endosome (Naughtin et al., 2010). MTMR4 is also reported to regulate BMP and TGFβ signaling pathway (Yu et al., 2010). Contribution of MTMR3 and MTMR4 to immunological disease is also reported. MTMR3 is a risk factor for inflammatory bowel diseases in which MTMR3 level is increased and PtdIns3P production is decreased. Reduction of PtdIns3P increases Caspase-1-dependent cytokines production and inflammation by inhibiting autophagy (Taguchi et al., 2010; Lahiri et al., 2015). MTMR4-dependent PtdIns3P production is required for *Salmonella*-mediated vacuole formation (Teo et al., 2016).

Although our previously laboratory found that PtdIns5P from PIKfyve is important for innate immune response to RNA virus infection (Kawasaki et al., 2013). Production of PtdIns from other phosphatase and kinase may be also contributed to the regulation of innate immune response. To further understand regulatory roles of innate immune response by PtdIns, I focused on MTMR3 and MTMR4 and analyzed their roles in innate immune response.

2. Materials and methods

2.1 Material

Cells

Cells that used in this study were described below:

1. HEK293 and HEK293T cells: human embryonic kidney cell line
2. HeLa cells: human cervix adenocarcinoma cell line
3. RAW264.7 cells: mouse macrophage cancer cell line
4. J774 cells: mouse macrophage monocyte cell line
5. Platinum-E (Plat-E): retroviral package cells
6. Bone marrow-derived macrophage (BMM): differentiated bone marrow cells induced by M-CSF
7. Bone marrow-derived dendritic cells (BMDC): differentiated bone marrow cells induced by GM-CSF
8. MEF cells: mouse embryonic fibroblast cells

Cells were cultured in Dulbecco's modified Eagle's medium (DMEM, Nacalai Tesque) supplemented with 10% heat-inactivated Fetal Bovine Serum (FBS, Life Technology) and Plat-E cells were cultured in DMEM containing 100 μM 2-mercaptoethanol (Nacalai), 1 μg / mL puromycin (Invivogen), 10 μg / mL Blasticidin (Invivogen) and 10% FBS at 37 °C in humidified 5% CO_2. Bone marrow cells were treated with 10 ng / mL M-CSF (Proteo Tech) or 10 ng / mL GM-CSF (Proteo Tech), 100 μM 2-mercaptoethanol, and incubated for 6 to 8 days at 37 °C and 5% CO_2 with Roswell Park Memorial Institute medium (RPMI) 1640 medium, Nacalai) containing 100 units / mL penicillin 100 μg / mL streptomycin (Nacalai) and 10% FBS to differentiate to BMM and BMDC, respectively.

Escherichia coli (*E. coli*)

E. coli (DH5α strain, TOYOBO) was used for transformation at the time of plasmid preparation. *E. coli* were cultured in LB medium (Nacalai) or LB agar plate (Nacalai) under 37 °C conditions.

Plasmids

Plasmids that I used were as follows:

1. Expression plasmids: pFLAG-CMV-2 (Sigma), pMX-IRES-puro retrovirus plasmid (Cell Biolabs, Inc), and pYpetC3

2. Luciferase reporter assay: pGL3-IFN-β-Luc, pSV40-Luc, and pTK-Luc
3. CRISPR/Cas9 system: pX330 plasmid that encoding Cas9 and pCAG-EGxxFP plasmid expressing EGFP as a reporter plasmid provided by Prof. Masahito Ikawa in Research Institute of Microbial Diseases, Osaka University.

Synthetic ligand and virus

1. Intracellular DNA Sensor = ISD + Lipofectamine 2000 (Life Technologies) = 2 μg : 2 μg
2. RLRs (RIG-I and MDA 5) = Poly I: C (Invivogen) + Lipofectamine 2000 (Life Technologies) = 2 μg : 2 μg
3. TLR 4 = gram negative bacterial cell wall component: lipopolysaccharide (LPS) 10 - 1000 ng / mL.
4. HSV-1 viruses

Sense and anti-sense ISD sequences were synthesized (Granier Japan) and annealed (sense, 5′TACAGATCTACTAGTGATCTATGACTGATCTGTACATGATCTACA). Poly I:C and LPS were purchased from Invivogen. Poly I:C and ISD were mixed with Lipofectamine 2000 (Life Technologies) at ratio 2:1 (μg:μl) in OptiMEM (Life Technologies) for stimulation.

Primer

Primers for sub-cloning and Real-Time PCR (RT-PCR) were designed based on mouse gene sequence from NCBI and ensemble (table 2). These primers were synthesis using greener bio-one, Eurofins, and Sigma.

The nucleotide primer that used are shown in table

Table 2. Primers sequences for MTMR3 and MTMR4 expression plasmid

Gene	Sequence (5'-3')	Restriction enzyme
pFLAG-MTMR3- Forward	atggatgaagagatgcggcatagccttg	EcoRI-
pFLAG-MTMR3- Reverse	tcagtttgaagtggcagcaataggcttatc	BamHI-
pFLAG-MTMR4- Forward	atgggtgaggagggccccccagcctgg	NotI-
pFLAG-MTMR4- Reverse	tcaactggaagccgtagcaatgggtttc	NotI-

Table 3. Primer Sequences for pFlag-CMV-2 analysis

Gene	Sequence (5'-3')
pFLAGCMV-sequence-forward	CGCAAATGGGCGGTAGGCGTG
pFLAGCMV-sequence-reverse	GCACTGGAGTGGCAACTTCC

Table 4. Primer sequences for quantitative real time PCR

Gene	Forward sequence (5'-3')	Reverse sequence (5'-3')
IFN-β	atggtggtccgagcagagat	ccaccactcattctgaggca
IL6	acaaccacggccttccctactt	cacgatttcccagagaacatgtg
r18S	gtaacccgttcaaccccatt	ccatccaatcggtagtagcg
mouse_MTM1	atcttaggaggatcgcaacg	taccgacaagaggctgactg
mouse_MTMR1	tccatttatgggagcagtga	tgcaccaatcttctccactc
mouse_MTMR2	agcagaaatggaggaaccag	cgctccatgctcttgaaata
mouse_MTMR3	tgggaatgtattctgctcca	caatgctggagcttgtagga
mouse_MTMR4	tgtgtcctggaaatgaaga	aaactgttcaggtggcttcc
mouse_MTMR6	ttccggtcctatcctactgc	tgaagcaaatgctcatcctc
mouse_MTMR7	ccagtttgggaacttcctgt	ggcagctcgattcttccaca
mouse_MTMR9	ggctctctgggtaccatcat	gagtggacaatgcctcaatg

Table 5. Primers sequences for pX330 construction to generate CRISPR/CAS9

Gene	Forward sequence (5'-3')	Reverse sequence (5'-3')
MTMR3-gRNA1	caccgcatagccttgagtgcatcc	aaacggatgcactcaaggctatgc
MTMR3-gRNA2	caccgttcctttccttgaacttca	aaactgaagttcaaggaaaggaac
MTMR4-gRNA1	cacctgaggagggccccccccagcc	aaacggctgggggggccctcctctcc
MTMR4-gRNA2	caccgggtgagggagtggaattcc	aaacggaattccactccctcaccc
MTMR3-gRNA-synthetic	gttcctttccttgaacttcatgg	
MTMR4-gRNA-synthetic	gggtgagggagtggaattcctgg	

Table 6. Primers sequences for pCAG-EGxxFP construction to generate CRISPR/CAS9

Gene	Forward sequence (5'-3')	Reverse sequence (5'-3')
MTMR3-pCAG	aaaggatccatggatgaagagatgcggcatagccttg	aagaattcctcttgtggataactaccacataatttg
MTMR4- pCAG	aaaggatccatgggtgaggagggccccccccagcctgg	aaagcggccgcgctctcctggctggcacaggtgggtatgc

Table 7. Primer sequence for MTMR3 and MTMR4 knockout cells analysis

Gene	Forward sequence (5'-3')	Reverse sequence (5'-3')
M13 - TOPO - seq	aaaggatccatggatgaagagatgcggcatagccttg	aaagaattcctcttgtggataactaccacataatttg
MTMR3-genotype	gtaagtaggcatggcagaagaatc	ctataaggctaaacacatattacac
MTMR4-genotype	cttggcttagttcacgtttccctgagta	aagccagggctctggtagatcctctaaa

Table 8. Primary and secondary antibody for confirming expression plasmid of MTMR3 and MTMR4

Antibody	Ratio dilution
anti-FLAG M2 mouse monoclonal antibody (Sigma)	1:1,000
anti-actin goat polyclonal antibody (I-19) (Santa Cruz)	1:1,000
antibody HRP-conjugated anti-Mouse IgG monoclonal antibody (Sigma)	1:30,000
antibody HRP-conjugated anti-Rabbit IgG (Sigma)	1:30,000

Table 9. Detail of sources and concentration of primary antibody for analyzing innate immune signaling

Antibody	Ratio dilution
anti-MTMR3 (Cell Signaling)	1:1,000
anti-MTMR4 (ABGENT)	1:1,000
anti-pIRF3 (Cell Signaling)	1:1,000
anti-IRF3 (Cell Signaling)	1:1,000
anti-pp65 (Cell Signaling)	1:1,000
anti-p65 (Cell Signaling)	1:1,000

Table 10. Detail of sources and concentration of primary and secondary antibody for immunofluorescence

Antibody	Ratio dilution
anti-FLAG M2 mouse monoclonal antibody (Sigma)	1:1,000
anti-actin goat polyclonal antibody (I-19) (Santa Cruz)	1:1,000
anti-calnexin (Santa Cruz)	1:100
anti-GM130 (BD Bioscience)	1:100

anti-EEA (BD Bioscience)	1:100
anti-Lamp-1 (Santa Cruz)	1:100
mouse-derived anti-IgG antibody labeled with Alexa 488	1:10,000
mouse-derived anti-IgG antibody labeled with Alexa 568	1:10,000
rabbit-derived anti-IgG antibody labeled with Alexa 488	1:10,000
rabbit-derived anti-IgG antibody labeled with Alexa 568	1:10,000
rabbit-derived anti-IgG antibody labeled with Alexa 647	1:10,000

Table 11. Primer sequence for generating stable cells of STING, MTMR3, MTMR4

Gene	Forward sequence (5'-3')	Reverse sequence (5'-3')
pMRX-IRES-Puro-pFLAG-MTMR3	aaaggatccgccaccatgggcggtaggcgtgtacggtgggag	aaagcggccgctcagtttgaagtggcagcaataggcta
pMRX-IRES-Puro-pFLAG-MTMR4	aaactcgaggccaccatgggtgaggagggccccccccagcc	aaagcggccgcttacgcacaagagttccgtagctgttca

Table 12. Primer sequence for generating expression of PH DOK-5 and PX $p40^{phox}$

Gene	Forward sequence (5'-3')	Reverse sequence (5'-3')
pMRX-IRES-Puro-PX $p40^{phox}$	aaaggatccgccaccatgggtgaggagggcccc	aaactcgagtcacatgatggccccttg
pMRX-IRES-Puro-PH DOK5	ggggaattcatggcttccaattttaatgacatagtga	aaagcggccgctcaggtccccacacactccatctggaga

Table 13. Primers sequence for sequencing retroviral plasmids

Gene	Forward sequence (5'-3')	Reverse sequence (5'-3')
pMRX-FLAG-puro-seq	caccgccctcaaagtagacggcatc	gacaaacgcacaccggccttattc
pCypet C3-seq	catggtcctgctggagttcgtg	gaaatttgtgatgctattgc

2.2 Methods

PCR

Nucleotide sequence information of each MTMR3 and MTMR4 gene was obtained from NCBI and primers were designed to amplify CDS sequences. Forward and reverse primers were designed with a restriction enzyme site (Table 2). PCR was carried out using mouse-derived cDNA as a template and KOD FX (TOYOBO) according to the manufacture procedure.

Electrophoresis and gel purification

PCR products were added 1/6-fold volume of 6x Loading buffer (TOYOBO) and were applied in 0.8% agarose gel with Midori Green (Japan Genetics). PCR products were electrophoresed at 100 V in TAE buffer (Nacalai). DNA bands in agarose gel were illuminated by the LED (Japan Genetics) and the target DNA fragment was cut out. PCR products were purified using illustra GFX ™ PCR DNA and GeLBand Purification Kit (GE Healthcare).

Ligation and transformation

pFLAG-CMV2 and PCR products were treated with selective restriction enzymes at 37°C for 60 minutes. After purifying the restriction enzyme-treated products, ligation reaction was carried out with 2 x Ligation Mix (TOYOBO) at 16°C for 30 minutes. The ligation product was

transformed to DH5α (TOYOBO), then plated on LB agar plate containing 50 μg / mL Ampicillin, and incubated overnight at 37 °C. The obtained colonies were inoculated in LB medium containing 50 μg / mL Ampicillin and *E. coli* were shaken overnight at 37 °C and 180 rpm/min. Amplified *E. coli* was collected by the centrifugation and plasmid extraction was performed using FastGene Plasmid Mini Kit (NIPPON Genetics). Insertion containing pFLAG-CMV2 vector were selected and performed sequencing analysis.

Sequence analysis

Sequence reactions were performed using Big Dye Terminator Ready Reaction Mix, 5 x Big Dye (ABI) by the indicated sequence primer. PCR reactions were performed at 95 °C for 1 minute, followed by 25 cycles at 95 °C for 10 seconds, 50 °C for 5 seconds and 60 °C for 4 minutes. The PCR products were precipitated by ethanol and the precipitants were added to HiDi Formamide (Applied Biosystem). The obtained DNA solution was heat-treated at 95 °C for 5 minutes and run in a capillary sequencer (Applied Biosystems 3130 x LG Genetic Analyzer). Sequence data was analyzed using GENETYX Ver. 19.01.1 (282).

Western blot of MTMR3 and MTMR4

pFLAG-MTMR3 and pFLAG-MTMR4 were transfected in HEK293 cells and the lysates were performed to Western blot (WB) using anti-FLAG antibody. Anti-Actin antibody was used as a loading control. Dilutions of the primary antibody were described in the Table 8

Cells were cultured in six well plates and lysed in a RIPA Buffer (50 mM Tris HCl, 150 mM NaCl, 0.5% Sodium deoxycholate, 1% Nonidet P-40, 0.1% Sodium dodecyl sulfate (SDS)). Lysates were centrifuged at 800 x g for 10 minutes and supernatants were used as a whole cell lysates. Whole cell lysates were mixed with 2 × SDS sample buffer (1 M Tris-HCl, 10% SDS, 20% Glycerol, 0.01% Bromophenol blue, 0.2 M Dithiothreitol) and heat-treated at 95 °C for 5 minutes. Samples were applied to 5-20% SDS polyacrylamide gel (ATTO) and electrophoresed in running buffer (0.25 M Tris, 1% SDS, 1.92 M Glycine) with 20 mA. Proteins were transferred to PVDF membrane (Bio-Rad) in transfer buffer (25 mM Tris, 20% Methanol, 1.92 mM Glycine) at 200 mA for 70 minutes. Transferred membranes were applied for blocking by TBST buffer (0.5 M Tris, 1.38 M NaCl, 0.027 M KCl, 0.05% tween 20) containing 5% skim milk for 1 hour at room temperature. Membranes were washed with TBST buffer for three times and incubated with the primary antibody diluted in TBST buffer containing 5% skim milk for overnight at 4 °C (table 9). Then, membranes were incubated with the secondary antibodies diluted in TBST buffer containing 5% skim at room temperature for 30 minutes. Membranes

were reacted with a luminescent reagent Western Lightning Plus-ECL (PerkinElmer) Enhanced Luminol Reagent and Oxidizing Reagent. The expressions of target protein were detected by Image Quant LAS-4000 (GE Healthcare).

Luciferase assay

Luciferase assay was done using a Dual-Luciferase Reporter Assay (Promega). pGL3-IFN-β-Luc which contained firefly luciferase gene downstream of the IFN-β promoter and pTK which contains Renilla luciferase gene downstream of TK promoter for internal control were used for the reporter assay. HEK293 cells or HEK293T cells were seeded on a 24 well plate and transfected with 500 ng expression plasmids together with 100 ng of pGL3 plasmids and 10 ng of pTK-SV40. Expression plasmids of MTMR3 and MTMR4 were used for the transfection with a concentration gradient of 125 ng, 250, ng and 500 ng. pFLAG-CMV-2 was used as mock. Expression plasmids and reporter plasmids were mixed and incubated with Polyethylenimine (Polysciences) in Opti-MEM (Gibco). After 15 minutes, the mixture was added to the cells, and medium was exchanged after 6 hours. On the next day, medium was removed and the cells were lysed with 100 μL of 5xPassive Lysis Buffer (Promega). Ten μL of cells lysates were added to a 96 well white plate. Each well was sequentially applied with 50 μL of Luciferase Assay Reagent II (Promega) and 50 μL of Stop & Glo Reagent (Promega), and the emission of firefly luciferase and Renilla luciferase was measured by Multi-mode plate reader TriStar LB 942 (Berthold).

Confocal microscopy

Cover glasses were prepared on a 24-well plate and were treated with Poly-L-lysine solution (Sigma) for seeding HEK293T and HeLa cells. The cells were stimulated with ISD (1μg/ml)-lipofectamine 2000 for various time points. Then, cells were washed with PBS and fixed with 4% paraformaldehyde (Nacalai Tesque) for 20 minutes at room temperature. After washing three times with 0.02% Triton X-100 in PBS, 100 mM glycine in 0.02% Triton X-100/PBS was added at room temperature for 30 minutes. Cells were washed 3 times with 0.02% Triton X-100 in PBS and were blocked with 10% FBS, 0.02% Triton X-100/PBS for 1h at room temperature. Cells were incubated with primary antibodies diluted with 10% FBS 0.02% Triton X-100 at 4 °C overnight. After washing three times with 0.02% Triton X-100, cells were applied with the secondary antibodies diluted with 10% FBS in 0.02% Triton X-100 and were incubated for 1 hour. After three times washing with 0.02% Triton X-100, Hoechst 33342 (Dojin) was

diluted with 10% FBS in 0.02% Triton X-100 and incubated for 10 minutes. After 3 times washing with 0.02% in Triton X-100, samples were enclosed on slide glasses with Fluoro-KEEPER Antifade Reagent, Non-Hardening Type (Nacalai Tesque). The prepared samples were observed with confocal fluorescence microscope LSM 700 (ZEISS), and images were processed with ZEN software. Dilution ratios of the primary and secondary antibodies are shown above (Table 10).

Preparation of pX330 for MTMR3 and MTMR4

Target sequences for Cas9/CRISPR in MTMR3 and MTMR4 were synthesized, and its forward and reverse primers were annealed with T4 PNK (New England Biolabs). Synthesized target DNA fragments were included and the kinase reaction was performed at 37 °C 15 min and annealing were performed at 95 °C 5 minutes, 65 °C 15 minutes, 60 °C 15 minutes, 55 °C 15 minutes, 50 °C 15 minutes, 45 °C 15 minutes and incubated on ice. Px330 was digested with BbsI and dephosphorylated FAST AP (Thermo Scientific) at 37 °C for 1 hour. Then, the plasmids were purified using illustra GFX ™ PCR DNA and GeL Band Purification Kit. The annealing product and BbsI-treated pX330 were ligated and transformed into DH5α. Plasmids were extracted from the obtained colonies, and sequence analysis was performed using pX330_sequence_Forward and shown in Table 5.

pCAG-EGxxFP-MTMR3 and pCAG-EGxxFP-MTMR4

PCR reactions were performed using pCAG-EGxxFP-MTMR3_Forward and pCAG-EGxxFP-MTMR3-Reverse for MTMR3, and pCAG-EGxxFP-MTMR4_Forward and pCAG-EGxxFP-MTMR4-Reverse for MTMR4 (Table 6). These primers were designed to amplify approximately 500 bp including CRISPR/Cas9 target sequence in the MTMR3 and MTMR4 sequence. PCR was performed using KOD FX. pCAG-EGxxFP and insert DNA were treated with restriction enzymes, and ligation, transformation, plasmid extraction, and sequence analysis were carried out in the same manner as above. pCAG-EGxxFP_Forward was used for sequence analysis.

pX330 and pCAG-EGxxFP electroporation into RAW264.7 cells and single cell sorting

Efficiencies of gRNAs were confirmed by co-transfection of pX330 and pCAG-EGxxFP in HEK293T cells. px330 (500 ng) and pCAG-EGxxFP (500 ng) were mixed with Polyethylenimine (Polysciences) and the mixture was incubated with HEK293T cells in 24 well plates. Cells were incubated for 1 day and were analyzed the efficiency of EGFP by Accuri C6.

High efficiency of target gRNA was used for generation of KO cells. px330 and pCAG-EGxxFP for MTMR3 and MTMR4 were electroporated into RAW264.7 cells. Cells and plasmids mixtures were prepared at 1×10^7 cells / 130 μl and 3 μg each of pX330 and pCAG-EGxxFP/tube in serum-free RPMI1640 medium. Subsequently, the mixtures were introduced into Neon Transfection System (ThermoFischer Scientific) under the conditions of 1680 V, 20 ms, and 2 Pulse. After seeded in a 3 cm dish and cultured for 2 days, cells were suspended with 200 μl of FACS buffer (PBS containing 1% BSA (Nacalai Tesque) and 2 mM EDTA (Nacalai Tesque)). The EGFP positive cells were sorted into a 96 well plate by FACS Aria (BD). Cells were cultured for around 2 weeks. When cell density was reached about 70%, cells were transferred to 24-well plates and analyzed genotype by sequencing analysis.

Generation of MTMR3/4 double KO cells

To obtain MTMR3 and MTMR4 double KO cells, RAW264.7 cells stably expressing Cas9/CRISPR were generated. Synthesized trans-activating CRISPR RNA (tracrRNA) and gRNA (or crRNA) were electroporated into the cells. One μl of 1.0 μg/ml crRNA and 3 μl of 0.5 μg/ml tracrRNA were mixed with 6 μl of cells suspension (1x 10^7/ml). RNA and cells mixture were subjected to electroporation by NEON at 1680 V and 20 msec. Electroporated cells were titrated and suspended to 96 well plate. Cells were cultured for around 2 weeks until cellular density reached 70%. Then, cells were transferred to 24 well plates and were isolated DNA for sequence analysis. In this method, almost 100 % of cells contained mutations in MTMR3 or MTMR4 gene.

Sequence genotyping of MTMR3 and MTMR4 KO RAW264.7 cells

RAW264.7 cells were lysed using 50 mM NaOH (Nacalai) and lysates were incubated at 95 °C for 1 hour and neutralized with 1 M Tris-HCl (pH 8.0) (Nacalai). Genomic region around Cas9/CRISPR target site was amplified by PCR using EX taq (TOYOBO). PCR reaction conditions were as follows: 95 °C 5 minutes in the first cycle, followed by 35 cycles of 95 °C 30 seconds, 50-60 °C 30 seconds and 72 °C 1 minute. PCR products were run by gel electrophoresis. The bands were cut and DNA was isolated by gel isolation kit. Then, TA cloning was performed using TOPO vector and inserts were analysis by sequencing. Sequence primers and PCR primer were shown in below table. The plasmid was constructed by the same cloning operation as above, and the mutation position was determined by comparing to genomic data of MTMR3 and MTMR4 (Table 7).

RNA isolation and cDNA synthesis

RNA was purified using TRIzol Reagent (Life technologies) following manufacture`s procedure. RNA was dissolved in 20 μL of RNase-free sterilized water (Nacalai Tesque) and the RNA concentration was measured by Nano drop. cDNA was synthesized using ReverTraAce (TOYOBO) from about 500 ng of RNA extracted from cells and/or tissue. The cDNA reaction solution was prepared according to the protocol of ReverTraAce and adjusted to 10 μL. Reaction conditions of reverse transcription were as follows: 30 °C for 10 minutes in the first cycle, followed by 42 °C for 1 hour and 99 °C for 5 minutes.

Expression analysis by Real-Time PCR

Real-Time PCR (RT-PCR) was performed using Power SYBR Green PCR Master Mix (Life Technologies) and Light Cycler 96 (Roche). The reaction solution was prepared according to the protocol of Power SYBR Green PCR Master Mix and adjusted to final volume 20 μL. The primers used are shown in Table. For the RT-PCR conditions, the first cycle was 95 °C for 10 minutes, followed by 40 cycles of 95 °C for 10 seconds and 60 °C for 1 minute. The ribosome 18S gene as an internal standard, the expression amount between tissues and cells was relatively evaluated by the ΔΔCt method.

Immunoprecipitation (IP) -WB of MTMR3 and MTMR4

Control and KO cells were cultured in 6 well plate and cells were lysed with IP-buffer (150 mM NaCl, 10 mM tris-HCL pH. 8, 10 mM EDTA, 2 mM EGTA, 0.2% tween 20). Lysates were applied with anti-MTMR3 or anti-MTMR4 antibody along with Protein A agarose beads (Thermo Fisher Scientific) and were rotated for o/n at 4 °C. Anti-body bounded Protein A beads were collected by spin down and washed three times with IP-buffer. Sample buffer was applied to the beads and samples were subjected to WB against anti-MTMR3 or anti-MTMR4 antibody. As an internal control, lysates were subjected to WB using anti-Actin antibody.

Induction of anti-viral innate immune response by PRRs ligand stimulation

Cells were stimulated with the indicated PRR ligand under the conditions shown below to induce an anti-viral innate immune response.

One μg of synthesized Poly I: C (Invivogen) was transfected into the cells together with the same concentration of Lipofectamin 2000. After stimulation, reaction was carried out for 6 hours.

Bacterial lipopolysaccharide (LPS) (Invivogen) 1 μg / ml was added to the culture supernatant. After stimulation, reaction was carried out for 2 hours.

Two μg of synthetic double-stranded DNA (Interferon Stimulatory DNA; ISD) (Greiner bio-one) was transfected into the cells together with an equivalent amount of Lipofectamin 2000. After stimulation, reaction was carried out for 6 hours.

Following each PRRs ligand reaction, RNA extraction and cDNA synthesis were carried out in the same manner as above, and the transcription level of type I IFN, IFN inducible gene IP-10 and inflammatory cytokine IL6 by Real-Time RT-PCR were measured.

ELISA assay

Protein levels of IL6, IP-10, and TNFα, in the culture supernatant were also measured according to the mouse DuoSet ELISA Development Kit (R&D). First antibody diluted with PBS was plated to a 96-well ELISA plate at 50 μL per well and incubated for overnight. On the next day, after washing with ELISA Wash Buffer [PBS containing 0.05% Tween 20 (Nacalai)], 200 μL of PBS containing 1% BSA was added to each well and blocking was carried out for 1 hour. After washing with ELISA Wash Buffer, each sample supernatant as well as the sample for preparing the eight calibration curves. At the same time, 50 μL was added to each well and allowed to react for 2 hours. After washing with ELISA Wash Buffer, 50 μL of Detection antibody diluted with 1% BSA-containing PBS was added to each well and reacted for 2 hours. After washing with ELISA Wash Buffer, it was labeled with Streptavidin-HRP diluted 140 times with PBS containing 1% BSA for 20 minutes. Wash with ELISA Wash Buffer, add equal 50 μL of each well of mixed solution of Staining solution and Substrate solution in ELISA POD Substrate TMB kit (Nacalai) to emit light, and determine the degree of luminescence of the control sample as a guideline was stopped with 25 μL of 1 M H 2 SO 4. The luminescence intensity was measured using an iMARK microplate reader (Bio-Rad), and IL6, IP-10 and TNFα protein concentrations contained in each sample supernatant were calculated using a calibration curve as standard.

WB analysis for innate immune signaling molecules

Cells cultured in six well plates were simulated with PRRs ligands such as ISD for 1h or 3h; Poly I:C for 1h or 3h; LPS for 15 min or 30 min. Cells were lysed and WB were performed as described above.

Stable cells expressing STING

Six μg of pMRX-STING-Flag-puro was transfected with 1 μg of pVSV-G (Addgene) to Plat-E cells which had been pre-cultured at 4 × 10^6 cells / 10 cm^2 dish. pMRX-STING-Flag-puro was mixed with an equal volume of Lipofectamine 2000 for 15 minutes for transfection in OptiMEM. Next day, the supernatants were changed to a fresh medium and cells were further incubated for 36 hours. Supernatants were path through a 0.22 μm filter and were transferred to RAW 264.7 cells which had been pre-cultured at 5 × 10^5 cells / 10 cm dish. Sixteen hours after the infection, supernatants were removed and medium was replaced to 4 μg/ mL puromycin containing DMEM. Expressions of STING were confirmed by WB and cellular staining by anti-Flag antibody.

Observation of YFP-PX $p40^{phox}$ and YFP-PH-DOK5

PX domain in $p40^{phox}$ and PH domain in DOK5 were amplified by PCR and sub-cloned into pYpetC3 vector. Mouse gene sequence data was obtained from NCBI and the primer sequences were attached restriction enzyme site (table). pCypetC3-PX $p40^{phox}$ and pCypetC3-PH DOK5 were electroporated into RAW 264.7 cells using NEON. The procedures were the same as described above. Cells were stained with antibodies against calnexin (endoplasmic reticulum), EEA (Early endosome) or GM130 (Golgi) (red). Cells were observed with fluorescence microscope LSM 700 (ZEISS) and the image was processed with ZEN software.

3. Results

I first assessed the expression pattern of MTM and MTMR family members in several cells such as RAW264.7 macrophage cells, murine bone marrow-derived dendritic cells (BMDCs), J774 macrophage-like cells, murine bone marrow-derived macrophages (BMMs) cells and murine embryonic fibroblast (MEFs) cells by RT-PCR. MTM family genes were widely expressed in all types of cells (Fig. 5 a, b). Among them, MTMR3 and MTMR4 have the FYVE domain that potentially binds to PtdIns and were also expressed in all type of cells. Our laboratory previously showed that PIKfyve regulates innate immune signaling by generating PtdIns5P production (Kawasaki et al., 2013). Thus, I focused on MTMR3 and MTMR4 and investigated whether they are involved in the regulation of innate immune signaling.

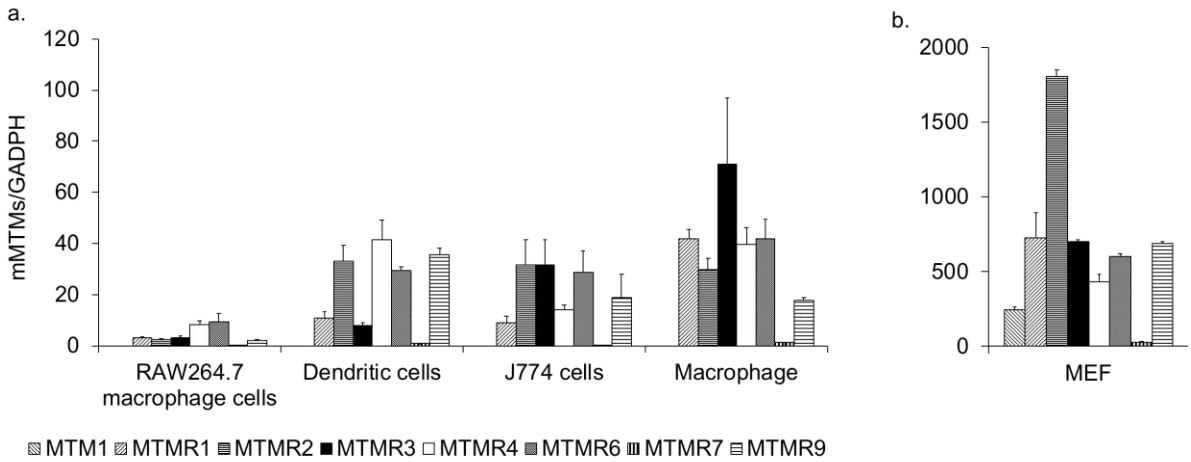

Fig. 5. Gene expression of MTM family members. (a, b) Expression of MTM1, MTMR1, MTMR2, MTMR3, MTMR4, MTMR6, MTMR7, MTMR9 in RAW264.7 cells, BM-DCs, J774 cells, BMMs (a) and MEF cells (b). were measured by RT-PCR**.** Data representative of at least two independent experiments.

I then examined the cellular localization of MTMR3 and MTMR4. I generated FLAG-tagged MTMR3 and MTMR4 expression plasmids and they were overexpressed in HeLa and HEK293 cells. Cells were stained with anti-FLAG antibody together with a marker protein; Calnexin (endoplasmic reticulum), EEA (early endosome) or GM130 (Golgi) (Fig. 6). Both MTMR3 and MTMR4 were distributed in the cytoplasm, but not colocalized with the organelle markers. Then, HEK293 cells were stimulated with ISD, a synthetic DNA that activates cGAS. ISD stimulation did not change MTMR3 and MTMR4 localization (Fig. 7).

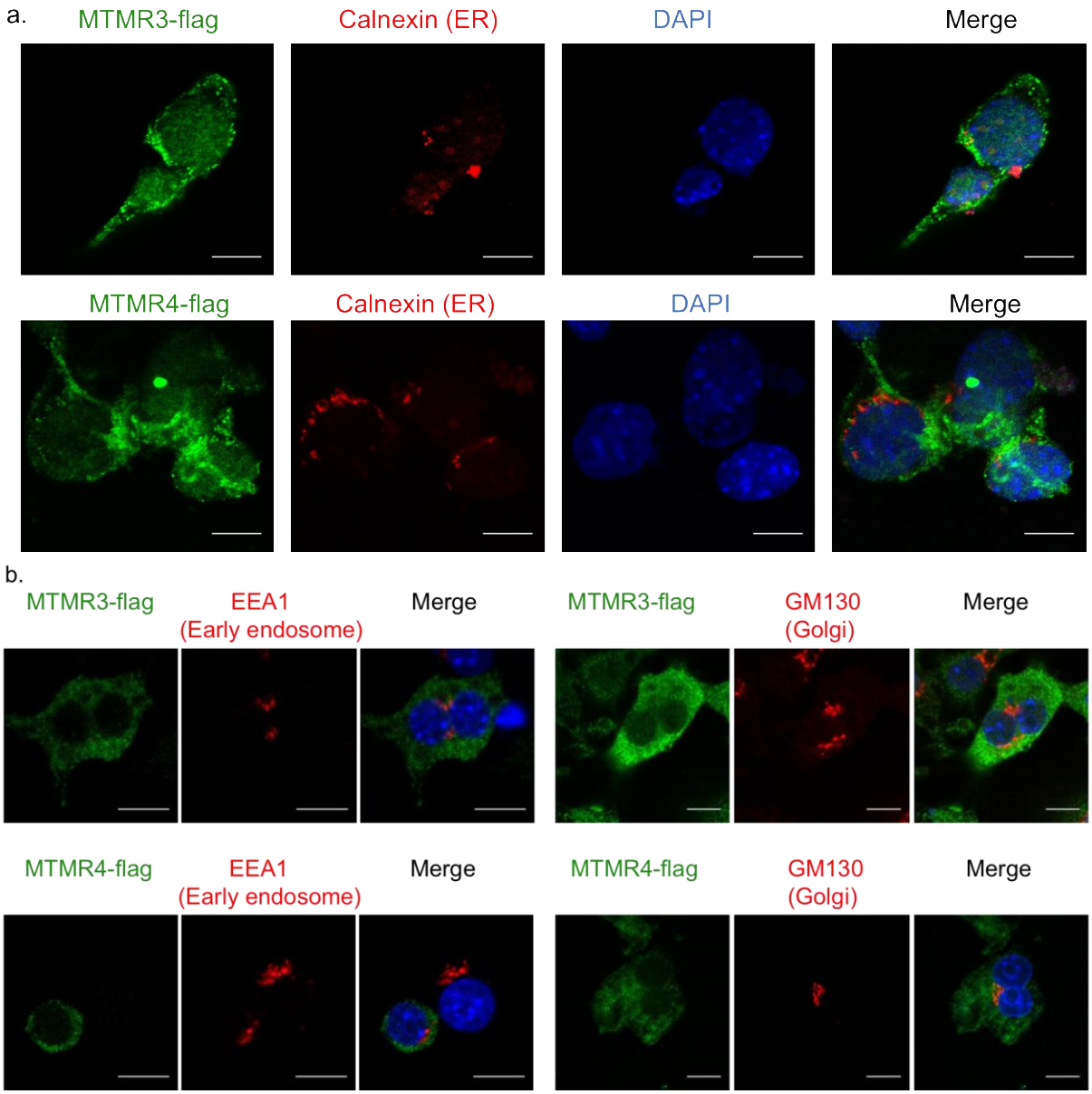

Fig. 6. Cellular localization of MTMR3 and MTMR4. HEK293 cells (a) or RAW264.7 cells (b, c) were transfected with MTMR3-flag and MTMR4-flag and were stained with Hoechst 33342 (blue), anti-FLAG (green) and the indicated antibodies; Calnexin (endoplasmic reticulum), EEA (early endosome) and GM130 (Golgi) (red). Data was representative of at least two independent experiments. Scale bar 10 μm

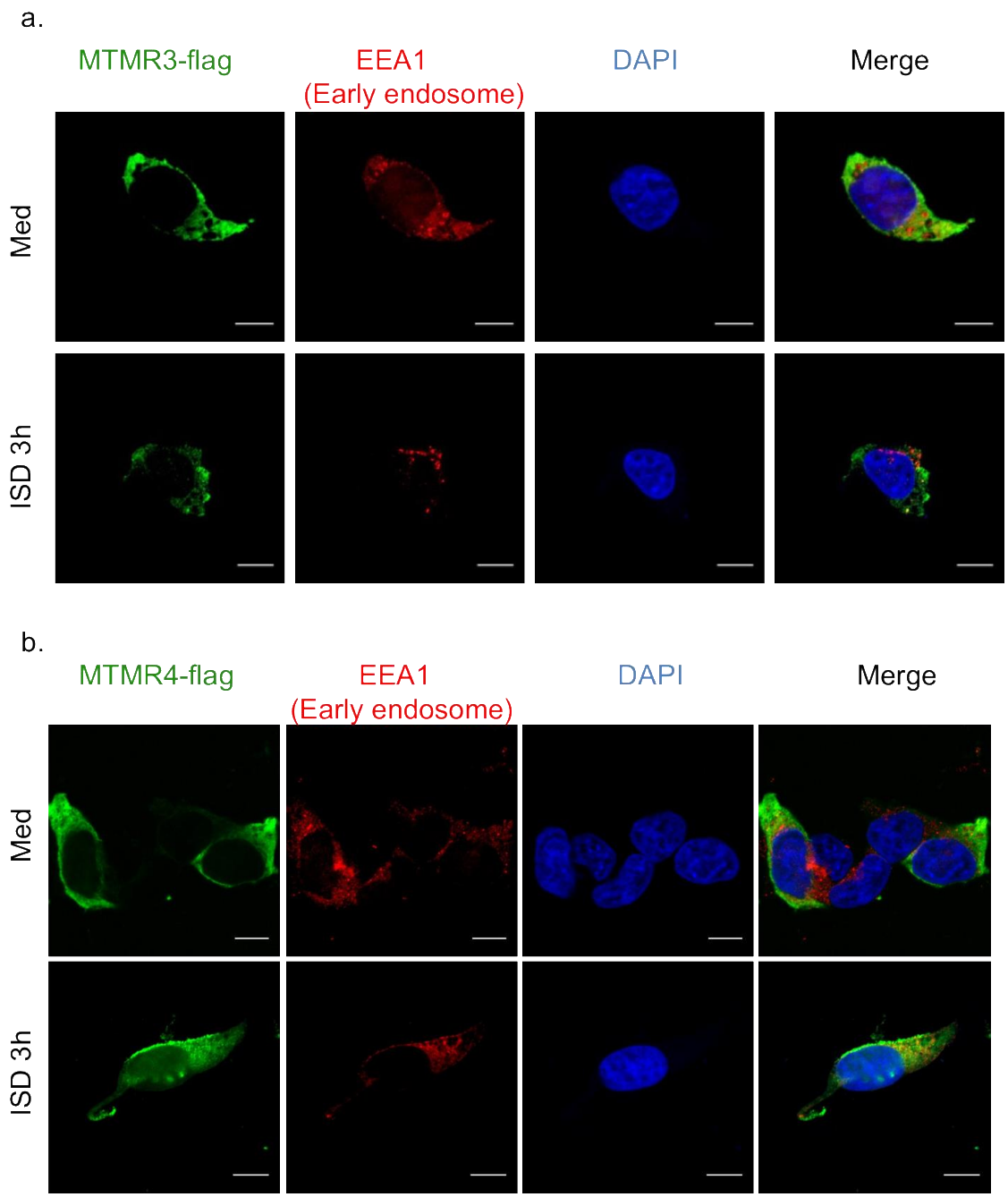

Fig. 7. Cellular localization of MTMR3 and MTMR4 after ISD stimulation. HeLa cells were transfected with MTMR3-flag (a) and MTMR4-flag (b) and stained with Hoechst 33342 (blue), anti-FLAG (green) and the indicated antibodies; Calnexin (endoplasmic reticulum), EEA (early endosome) and GM130 (Golgi) (red). Data representative of at least two independent experiments. Scale bar 10 μm

Next, to understand the contribution of MTMR3 and MTMR4 to innate immune signaling, I performed a reporter assay for IFNβ promoter. MTMR3 and MTMR4 expression plasmids were overexpressed together with a luciferase reporter plasmid driven by the IFNβ promoter in HEK293T cells. I found that overexpression of either or both MTMR3 and MTMR4 did not influence IFNβ promoter activity (Fig. 8 a). Then, I co-overexpressed MTMR3 and/or MTMR4 along with an adaptor protein STING, IPS-1, MyD88 or TRIF, which is

involved in cGAS, RLRs, all TLRs excepted for TLR3 or TLR3 signaling, respectively, into HEK293T cells. Expression of the adaptor protein alone significantly increased the promoter activity. However, STING-induced promoter activity was reduced by co-expression with MTMR3/4 in comparison with others adapters (Fig. 8 b-e). These results suggest that MTMR3/4 regulates STING-mediated DNA sensing pathway.

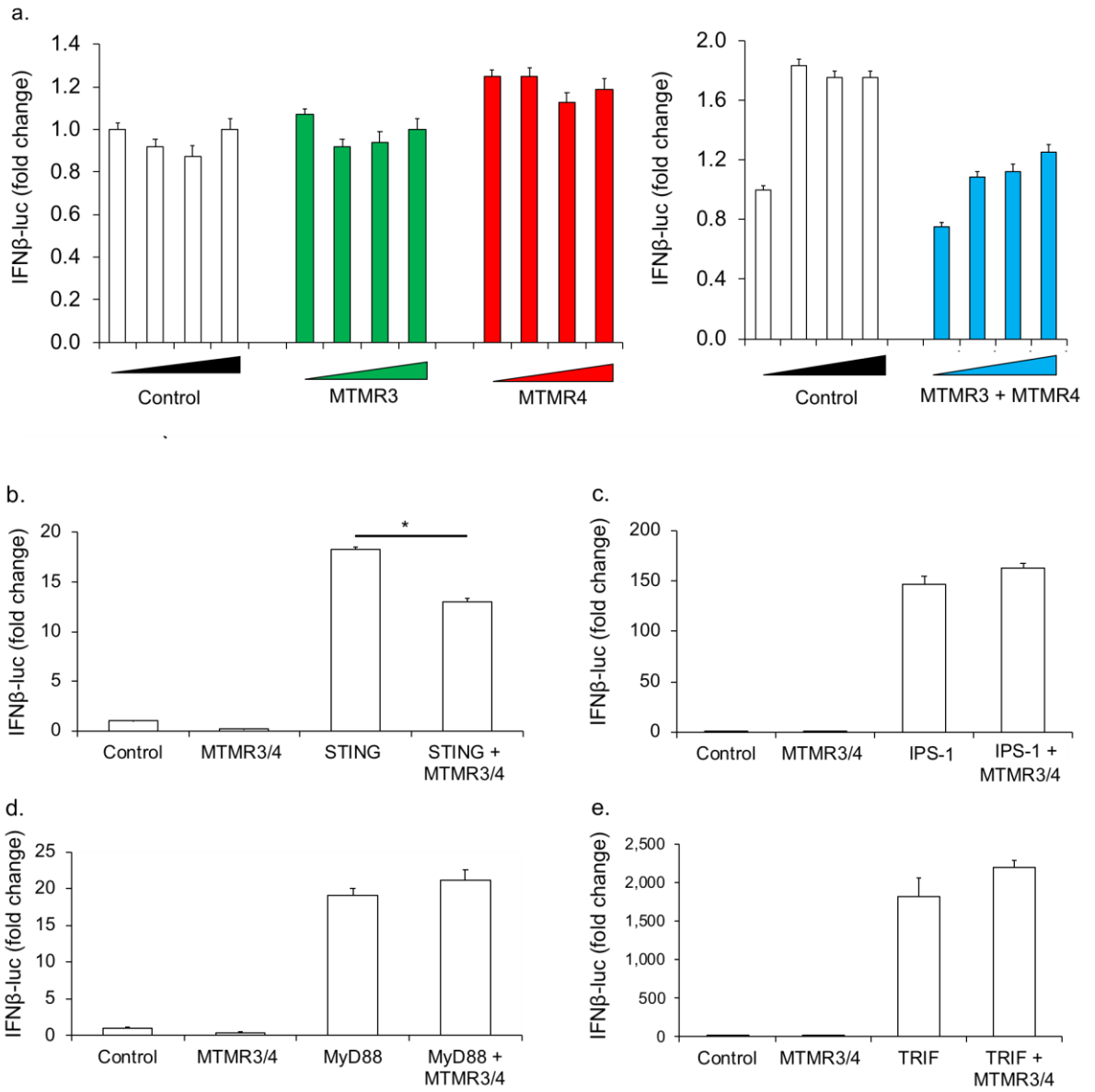

Fig. 8. IFNβ promotor assay by MTMR3/4 expression. (a) HEK293T cells were transfected with pFLAG-MTMR3 and/or pFLAG-MTMR4 with pGL-Ifnb-luc. (b-e) HEK293T cells were co-transfected with pFLAG-MTMR3 and pFLAG MTMR4 together with an adaptor protein STING (b), IPS-1 (c), MyD88 (d) or TRIF (e). After 24h from transfection, cells were lysed and luciferase reporter activity was measured. Data are expressed as means ±SEM, n=3 per group. *P < 0.05, ***P <0.01, one-way Anova with correction provide by Tuckey's multiple comparisons test.

3.1 MTMR3 is dispensable for innate immune signaling

To understand the physiological function of MTMR3 and MTMR4 in innate immune responses, I generated MTMR3 knockout (KO) RAW264.7 cells by using CRISPR/Cas9 system. I designed gRNA in exon 3 regions that contained the PH Gram domain. Target DNA sequences for Cas9 were sub-cloned into px330 plasmid that expresses hCas9 and trans activating CRISPR RNA (tracrRNA). gRNA is located next to PAM sequence (NGG) and 20bp sequence which potentially shows low off-target effects that do not cross react with others site in genome. To monitor double stand break (DSB) in transfected cells, I sub-cloned exon3 containing gRNA binding DNA fragment into pCAG-EGxxFP plasmid which induces expression of GFP signal by DSB of target sequence. GFP positive cells are expected to acquire DSB of target sequence in genomic region. I evaluated efficiency of gRNA sequence by co-transfection of px330 and pCAG-EGxxFP into HEK293T cells and GFP signals were monitored by FACS analysis after 24h transfection. High efficacy of guide sequence was selected for the generation of KO cells (Fig. 9 a).

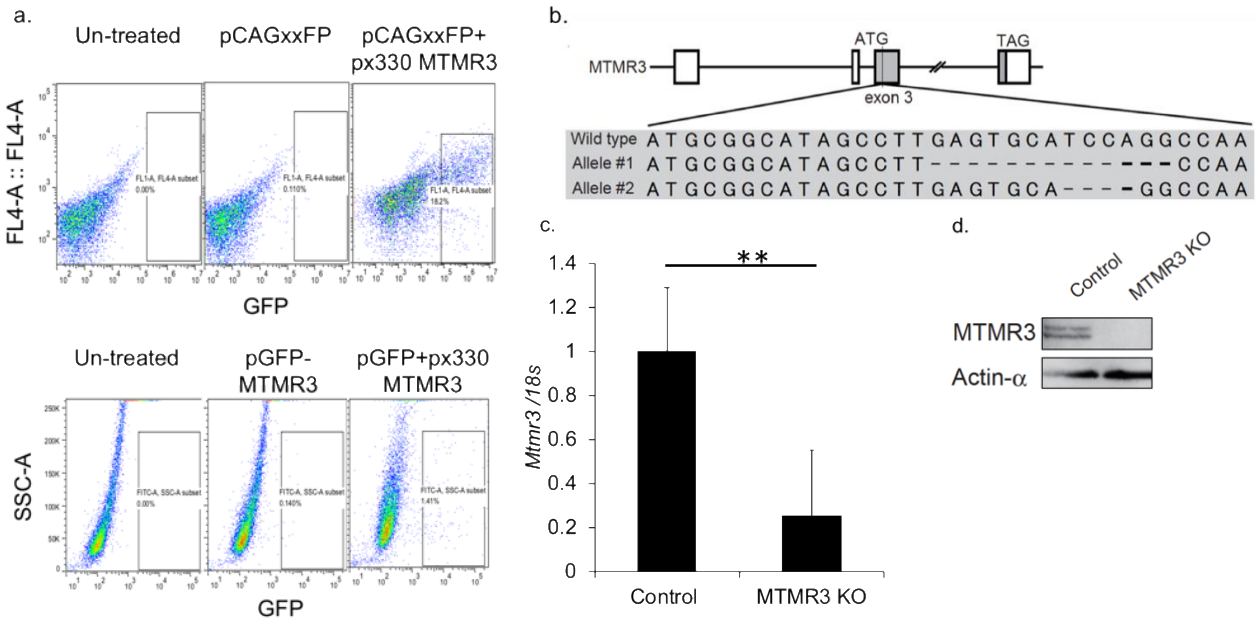

Fig. 9. Generation of MTMR3 KO cells. (a) HEK293T cells (upper) and RAW264.7 cells (lower) were transfected with px330 and pCAG-EGxxFP and analyzed by FACS. GFP positive cells in RAW264.7 cells were sorted out and cultured. (b) Comparison of genomic sequences of isolated cells. (c) Expression of MTMR3 in control and MTMR3 KO cells was analyzed by RT-PCR (d) Expression of MTMR3 in control and MTMR3 KO cells were annualized by IP-WB. Data are expressed as means ±SEM, n=3 per group. *P < 0.05, ***P <0.01,

I transfected px330 and pCAG-EGxxFP for MTMR3 in RAW264.7 cells (Fig. 9 a) and GFP positive cells were sorted to 96 well plate. After cells were grown, genomic DNA of exon 3 in MTMR3 was amplified by PCR and PCR fragments were sub-cloned into TOPO vector. Then, frame sifted mutations were verified by sequencing analysis. MTMR3 KO cells showed

16bp and 4bp deletion in each allele (Fig. 9 b). I checked expression of *MTMR3* by real-time PCR, and the expressions were significantly lowered in MTMR3 KO cells (Fig. 9 c). I performed immunoprecipitation-WB (IP-WB) using anti-MTMR3 and confirmed a loss of MTMR3 protein expression in MTMR3 KO cells (Fig. 9 d).

Next, I stimulated control and MTMR3 KO RAW264.7 cells with ISD, Poly I:C (RLRs ligand) and LPS (TLR4 ligand) and measured *Ifnb, Il6, Cxcl10* and *Tnfa* mRNA by RT-PCR. Expression of these genes was comparable between control and MTMR3 KO cells (Fig. 10 a-d). I also measured production of IL6, CXCL10 and TNFα in the culture supernatant by ELISA, but these cytokines production was also comparable between control and MTMR3 KO cells (Fig. 11 a-c). Next, I investigated IRF3 and p65 (NF-κB) phosphorylation after these stimulations. Consistent with cytokines and type I IFNs expression, IRF3 and p65 phosphorylation was also comparable between control and MTMR3 KO cells (Fig. 12). These results suggest that MTMR3 is dispensable for cytokine expression induced by cGAS, RLRs and TLR4.

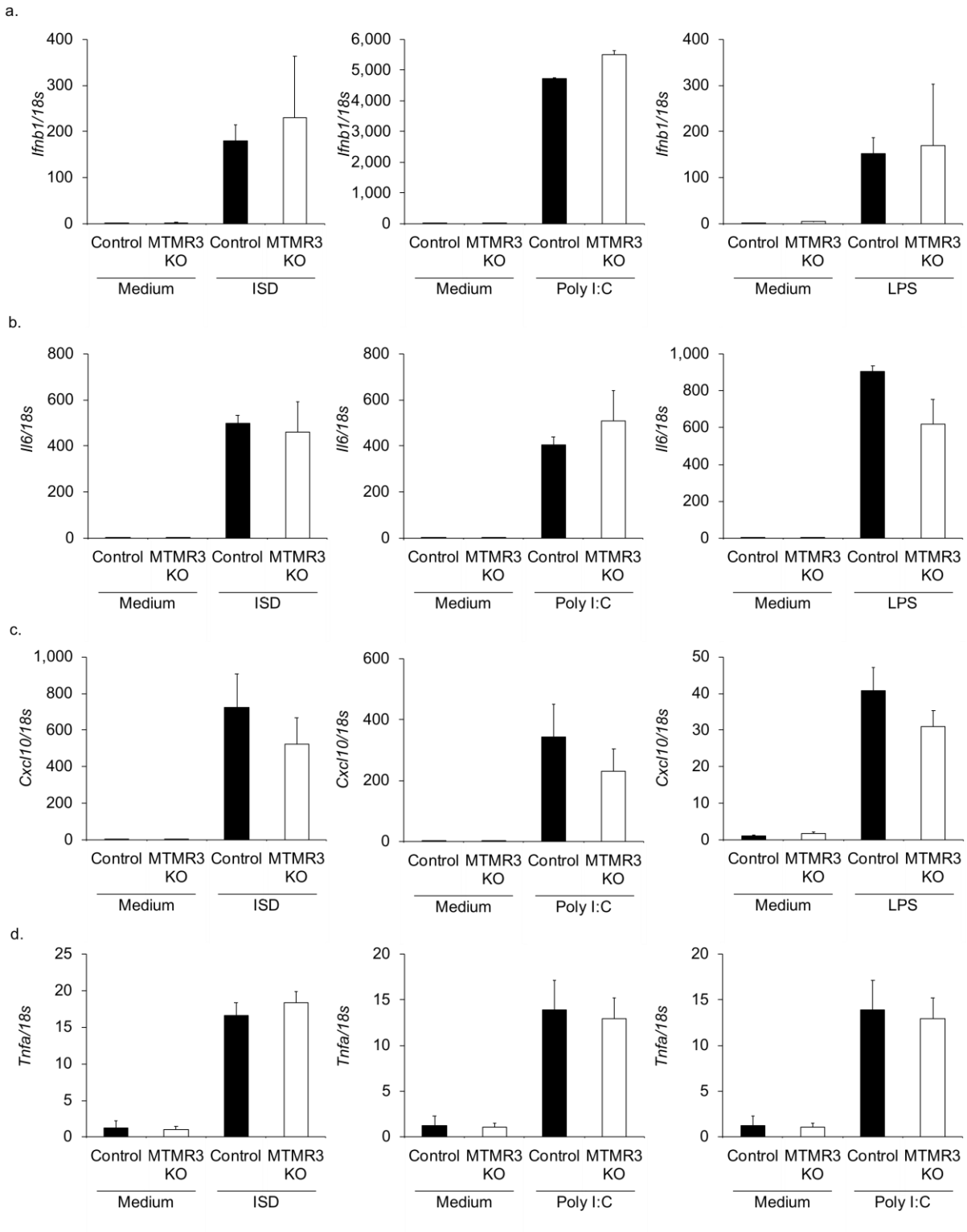

Fig. 10. Cytokines genes expression after innate immune stimulation in MTMR3 KO cells. Control and MTMR3 KO cells were stimulated with ISD, Poly I:C and LPS. Expression of *Ifnb* (a), *Il6* (b), *Cxcl10* (c) and *Tnfa* (d) were measured by RT-PCR

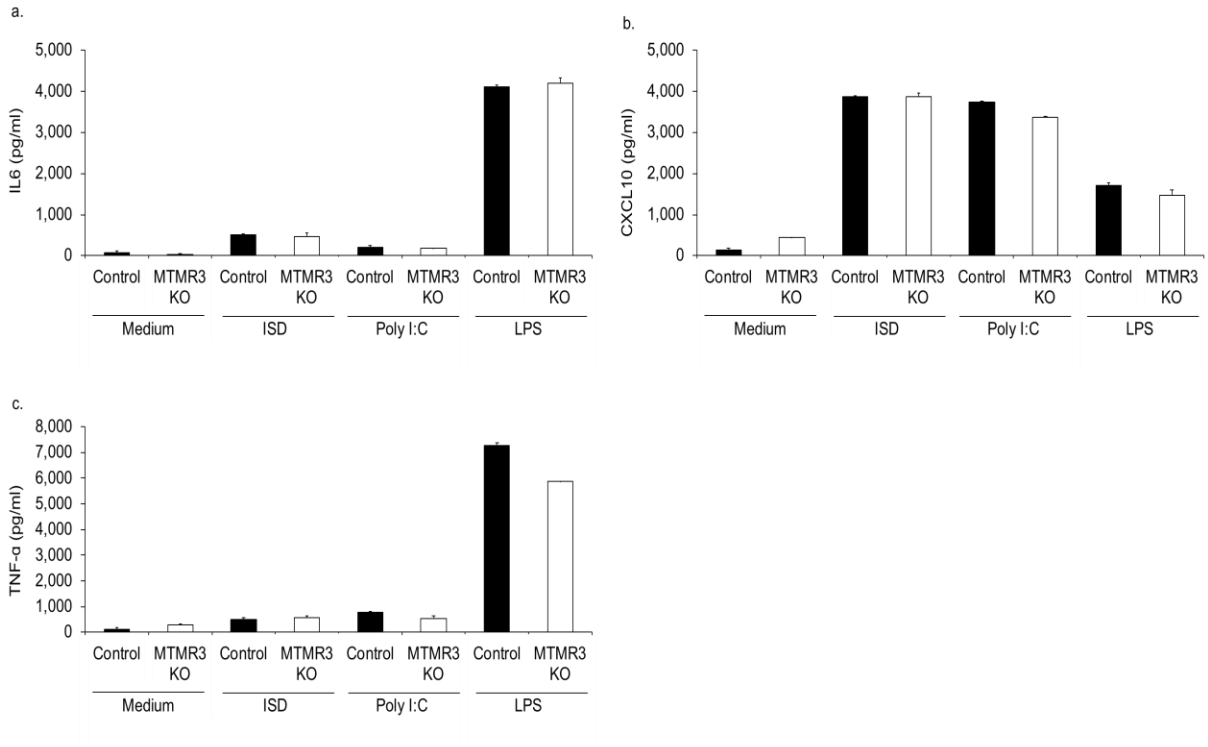

Fig. 11. Cytokines production after innate immune stimulation in MTMR3 KO cells. Control and MTMR3 KO cells were stimulated with ISD, Poly I:C or LPS for 24h. IL6, CXCL10 and TNFα production was measured by ELISA.

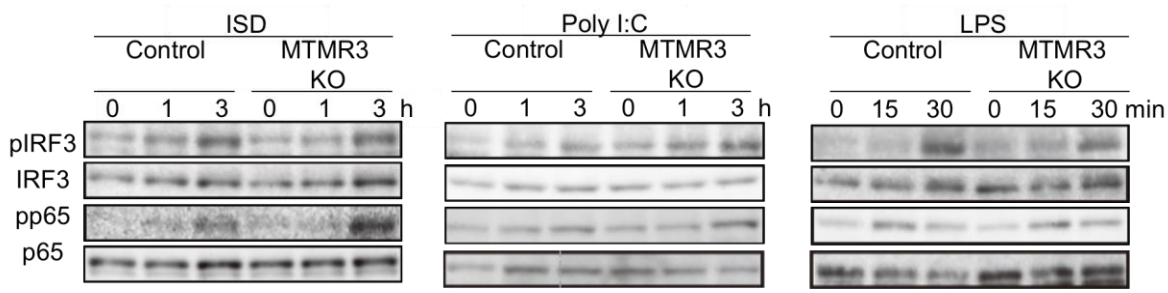

Fig. 12. Phosphorylation of transcription factor after innate immune stimulation in MTMR3 KO cells. Control and MTMR3 KO cells were stimulated with the indicated time points and were analyzed IRF3 and p65 phosphorylation by WB.

3.2 MTMR4 is dispensable for innate immune signaling

Next, I generated MTMR4 KO RAW264.7 cells by using the same strategy with MTMR3 KO cells generation. I designed the gRNA at the exon 3. I isolated MTMR4 KO cells that have 4bp homozygous mutation (Fig. 13 a, b). I examined the level of MTMR4 by real-time PCR and found that MTMR4 KO cells showed reduced *MTMR4* mRNA expression (Fig. 13 c). IP-WB analysis using anti-MTMR4 antibody clearly showed a loss of MTMR4 protein expression in MTMR4 KO cells (Fig. 13 d).

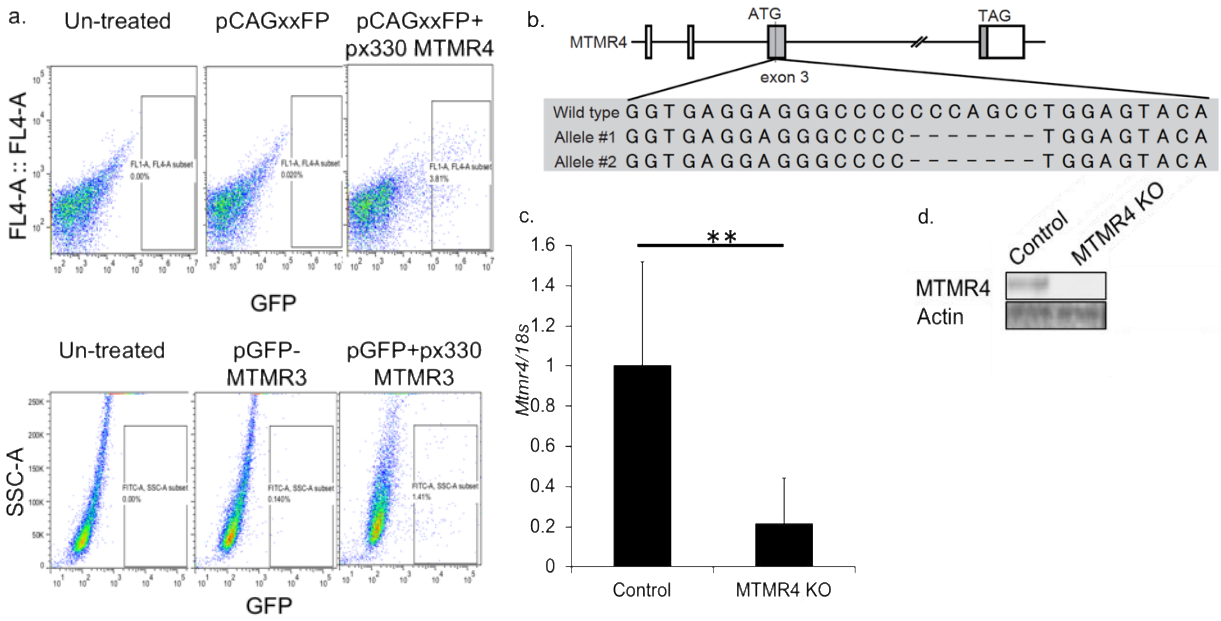

Fig. 13. Generation of MTMR4 KO cells. (a) HEK293 cells (upper) and RAW264.7 cells (lower) were transfected with px330 and pGxxFP and analyzed by FACS. GFP positive cells in RAW264.7 cells were sorted out and cultured. (b) Comparison of sequences of isolated cells. (c) Expression of MTMR4 in control and MTMR4 KO cells was analyzed by RT-PCR (d) Expression of MTMR4 in control and MTMR4 KO cells were annualized by IP-WB Data are expressed as means ±SEM, n=3 per group. *P < 0.05, ***P <0.01,

Ifnb, *Il6*, *Cxcl10* and *Tnfa* mRNA expression after ISD, Poly I:C and LPS was comparable between control and MTMR4 KO cells (Fig. 14 a-d). Moreover, IL6, CXCL10 and TNFα production was also unimpaired in MTMR4 KO cells (Fig. 15 a-c). IRF3 and p65 phosphorylation was also comparable between control and MTMR4 KO cells (Fig. 16). These results suggest that MTMR4 is also dispensable for the regulation of innate immune responses.

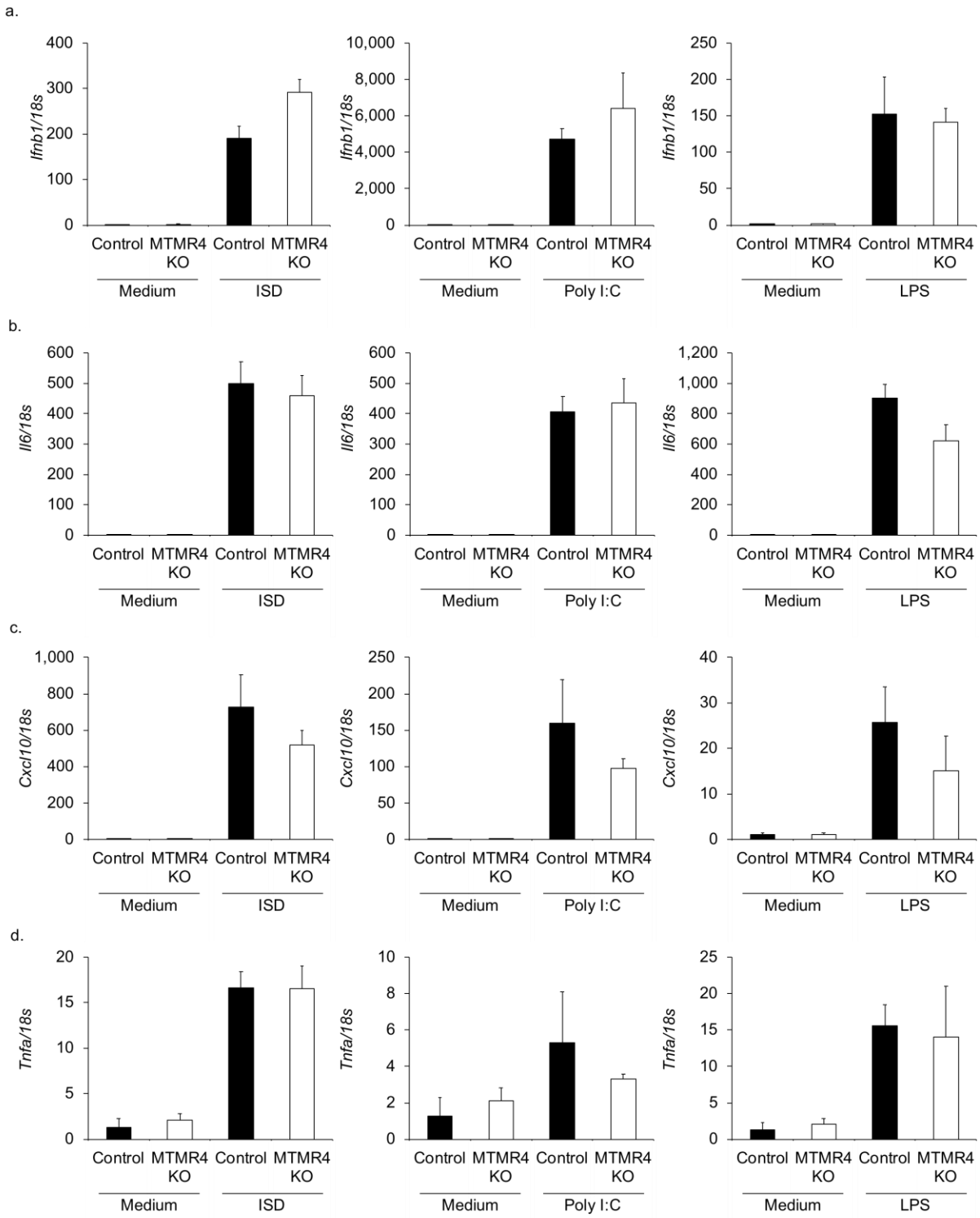

Fig. 14. Cytokines genes expression after innate immune stimulation in MTMR4 KO cells. (a-d) Control and MTMR4 KO cells were stimulated with ISD, Poly I:C and LPS. Expression of *Ifnb* (a), *Il6* (b), *Cxcl10* (c) and *Tnfa* (d) was measured by RT-PCR.

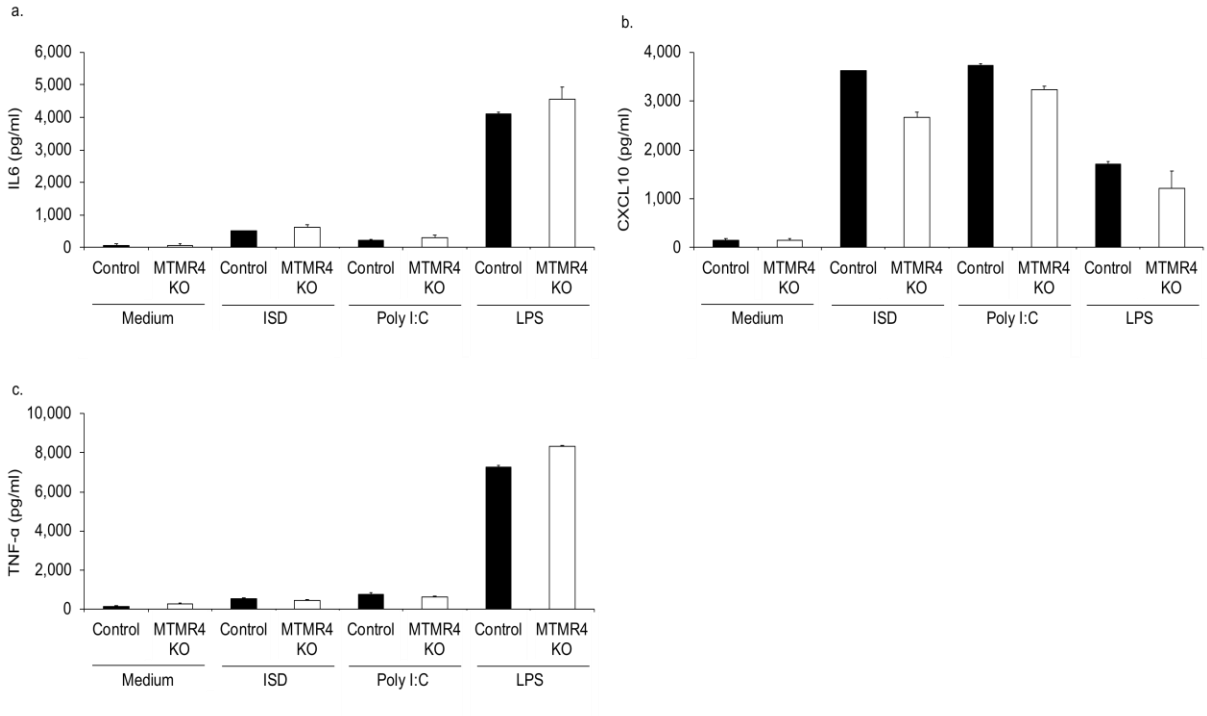

Fig. 15. Cytokines production after innate immune stimulation in MTMR4 KO cells. Control and MTMR4 KO cells were stimulated with ISD, or LPS for 24h. IL6, CXCL10 and TNFα production was measured by ELISA.

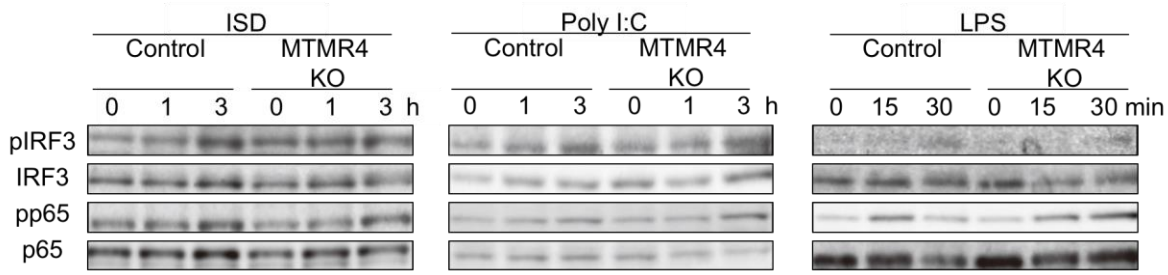

Fig. 16. Phosphorylation of transcription factor after innate immune stimulation in MTMR4 KO cells. Control and MTMR4 KO cells were stimulated with the indicated time points and were analyzed IRF3 and p65 phosphorylation by WB.

3.3 MTMR3/4 require for DNA sensing innate immune response

Either MTMR3- or MTMR4-deficiency did not influence innate immune responses. MTMR3 and MTMR4 have similar secondary structure and overlapped expression patterns in various cells as tested, suggesting the possibility that they may have complementary functions. I therefore generated MTMR3/MTMR4 double KO (DKO) RAW264.7 cells using CRISPR/CAS9 system. To increase the efficacy of mutations in both alleles in two genes together, the strategy for generating DKO cell was modified. CRISPR RNA (crRNA) having gRNA was synthesized and crRNA was transfected to RAW264.7 cells stably expressing Cas9 and tracrRNA. crRNA-transfected cells were then titrated to one cell and cultured for growth. Then, gRNA target region in MTMR3 and MTMR4 were amplified by PCR and PCR fragments

were sequenced. Isolated cells having frameshift mutation in both alleles in both MTMR3 and MTMR4 region were shown in Fig. 17 a. Deficiency of these genes was confirmed by RT-PCR and IP-WB against anti-MTMR3 and anti-MTMR4 antibodies (Fig. 17 b, c).

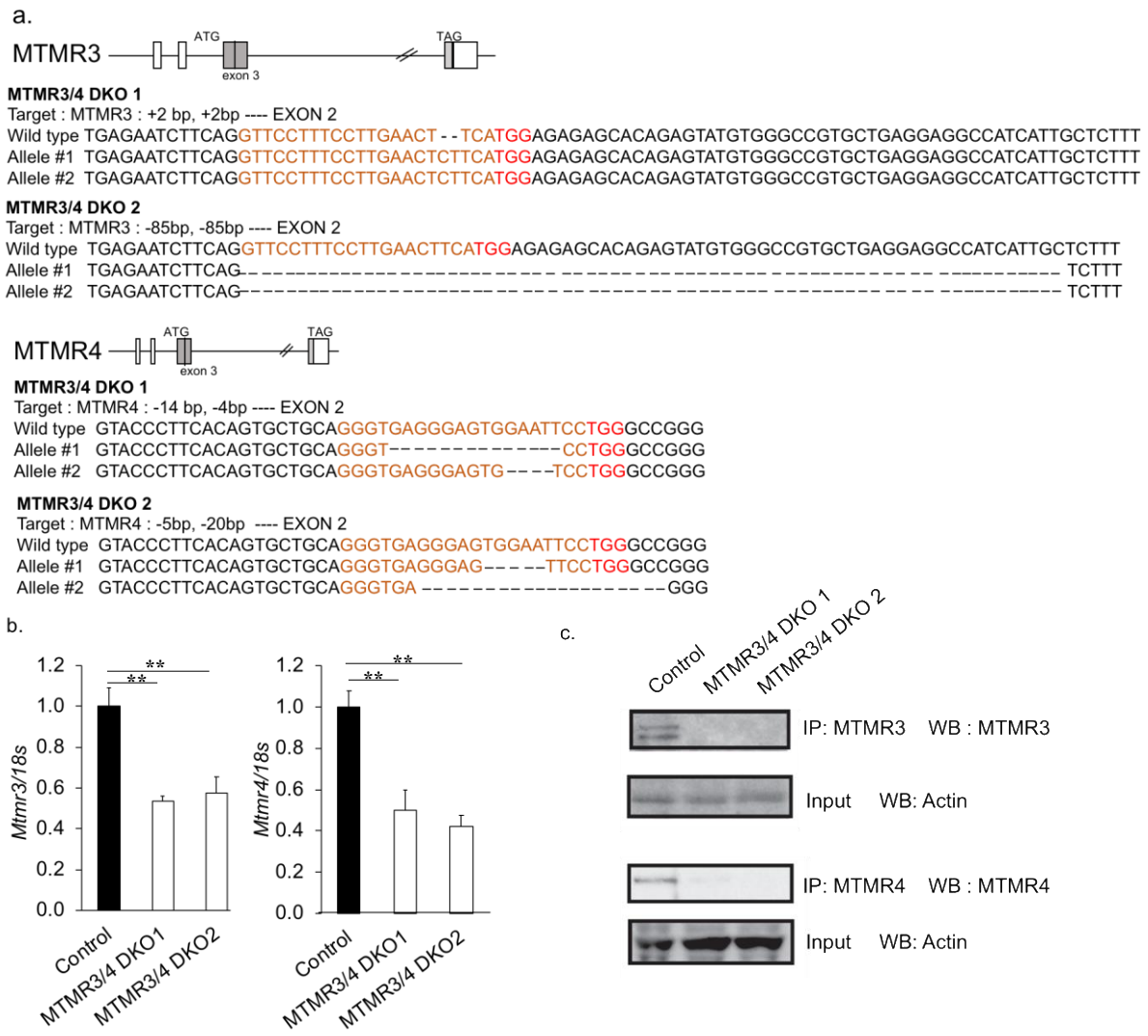

Fig. 17. Generation of MTMR3/4 DKO cells. (a) Comparison of genome sequences of isolated cells. (b) Expression of MTMR3 and MTMR4 were analyzed by RT-PCR (c) Expression of MTMR3 and MTMR4 was analyzed by IP-WB.

I stimulated control and two different lines of MTMR3/4 DKO (DKO1 and DKO2) cells with ISD, Poly I:C and LPS and measured cytokine mRNA. Interestingly, *Ifnb*, *Il6*, *Cxcl10*, but not *Il10* expression after ISD stimulation was significantly increased in both MTMR3/4 DKO1 and DKO2 compared to control cells. On the other hand, *Ifnb*, *Il6* and *Cxcl10* expression after Poly I:C and LPS stimulation was comparable (Fig. 18). Consistent with gene expression, IL6, CXCL10 and TNFα production was also significantly increased in MTMR3/4 DKO cells after stimulation with ISD, but not with Poly I:C and LPS (Fig. 19). IRF3 phosphorylation after ISD

stimulation was also increased in both MTMR3/4 DKO1 and MTMR3/4 DKO2 cells compared to control cells whereas IRF3 phosphorylation after and LPS stimulation was unimpaired (Fig. 20). These results suggest that both MTMR3 and MTMR4 negatively regulate DNA-mediated innate immune responses.

To further support MTMR3/4 function in DNA sensing innate immune responses, control and MTMR3/4 DKO1 cells were infected with DNA virus; Herpes Simplex Virus-1 (HSV-1). *Ifnb* expression in MTMR3/4 DKO1 was higher than in control cell (Fig. 21). These results also support that MTMR3 and MTMR4 together are essential in host defensive responses against DNA viruses.

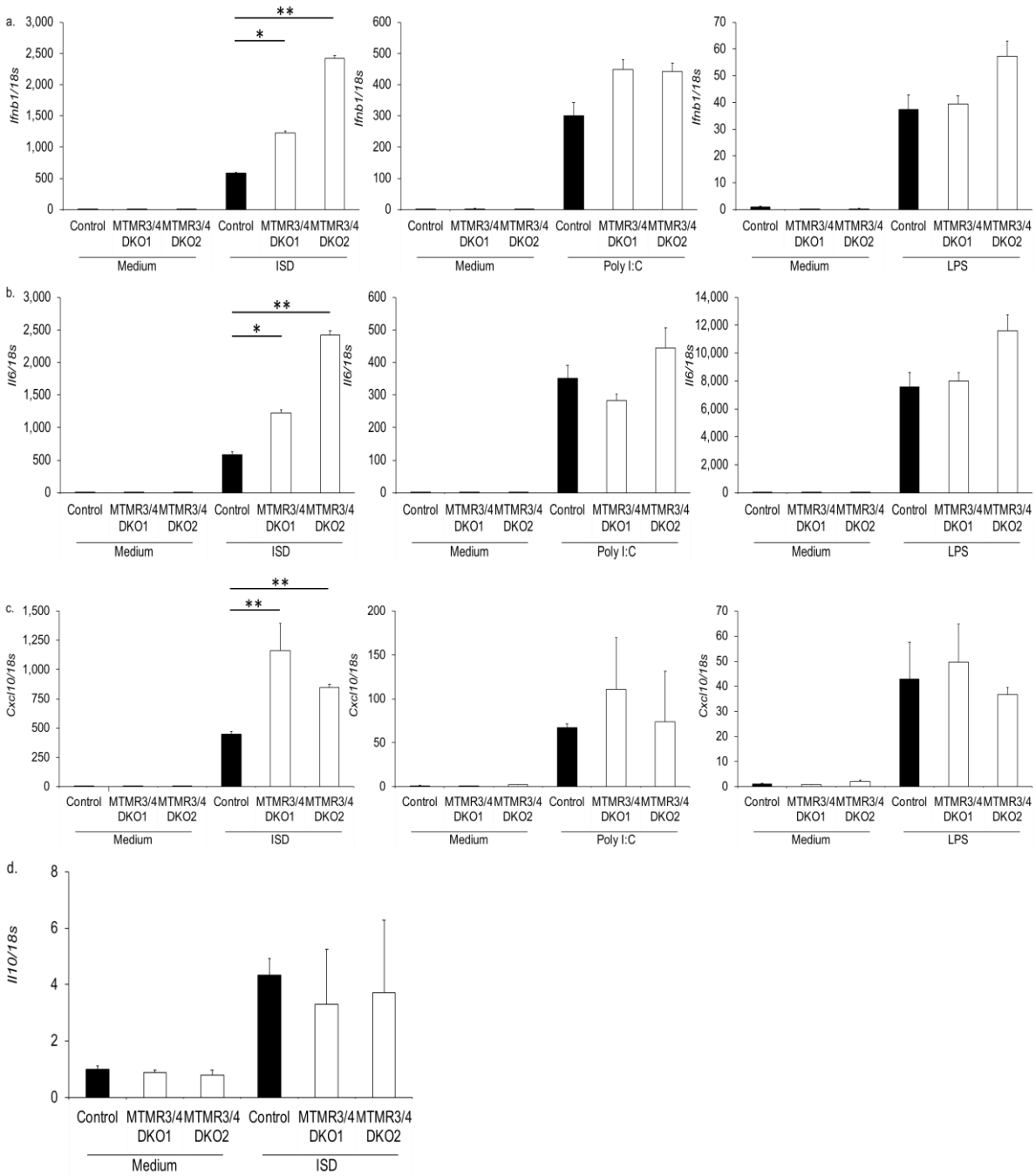

Fig. 18. Cytokines genes expression after innate immune stimulation in MTMR3/4 DKO cells. Control and MTMR3/4 DKO cells were stimulated with ISD, Poly I:C or LPS. mRNA for *Ifnb* (a), *Il6* (b), *Cxcl10* (c) *and Il10* (d) were measured by RT-PCR.

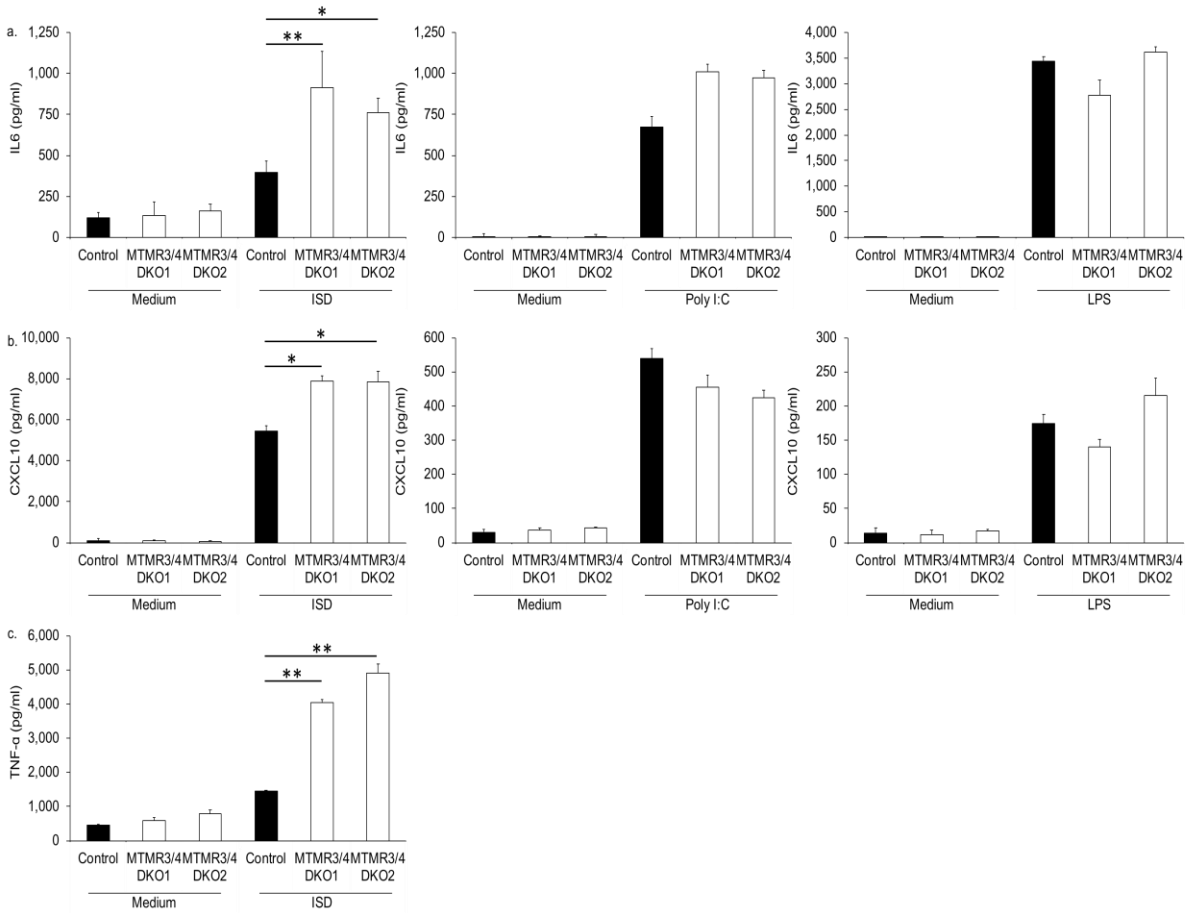

Fig. 19. Cytokines production after innate immune stimulation in MTMR3/4 DKO cells. Control and MTMR3/4 DKO cells were stimulated with ISD, Poly I:C or LPS for 24h. IL6 (a), CXCL10 (b) and TNFα (c) production was measured by ELISA.

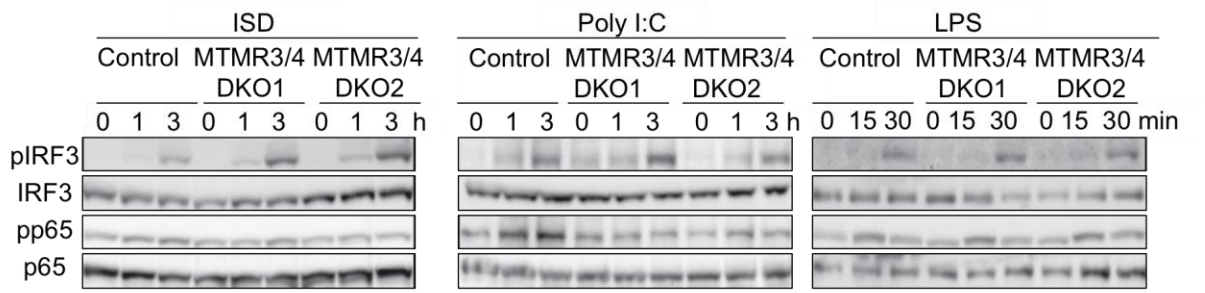

Fig. 20. Phosphorylation of transcription factor after innate immune stimulation in MTMR3/4 DKO cells. Control and MTMR3/4 DKO cells were stimulated with ISD, Poly I:C or LPS for the indicated time points. Cells lysates were subjected to WB analysis with the indicated antibodies

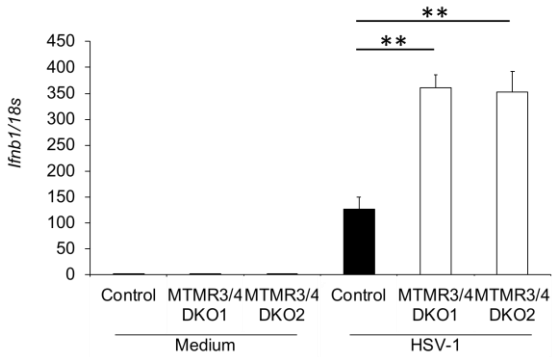

Fig. 21. *Ifnb* expression by HSV-1 infection in MTMR3/4 DKO cells. Control and MTMR3/4 DKO cells were infected with HSV-1 and *Ifnb* expression was measured by RT-PCR

3.4 The PtdIns3P and PtdIns5P localization

MTMR3 and MTMR4 are shown to dephosphorylate PtdIns(3,5)P_2 and PtdIns3P, and generate PtdIns5P and PtdIns, respectively. MTMR3/4-deficiencies are therefore expected to reduce the production of PtdIns5P and/or increase the production of PtdIns3P. To monitor cellular distribution of PtdIns5P and PtdIns3P, I expressed YFP-tagged PX domain in $p40^{phox}$ (YFP-PX $p40^{phox}$) and YFP-tagged PH domain in DOK5 (YFP-PH DOK5), which binds to PtdIns3P and PtdIns5P, respectively, in RAW264.7 cells (Kanai et al., 2001; Favre et al., 2003; Lemmon, 2008; Ellson and Yaffe et al., 2009). Both YFP-PX $p40^{phox}$ and YFP-PH DOK5 showed puncta structures in the cells (Fig. 22). To further understand cellular localization of YFP-tagged these markers, the cells were co-stained with a series of organelle maker; EEA1(early endosome), GM130 (Golgi), Calnexin (ER) or LAMP1 (Lysosome). YFP-PX $p40^{phox}$ localized mainly in the lysosome and partially in the endosome whereas YFP-PH DOK5 localized in unclear endosomal membrane and lysosome (Fig. 22). I then expressed YFP-PX $p40^{phox}$ and YFP-PH DOK5 in MTMR3/4 DKO cells and compared cellular distribution. YFP-PX $p40^{phox}$ expression in MTMR3/4 DKO cells showed increased YFP positive dot-like structures compared to control cells whereas YFP-PH DOK5 expression did not show differences in the cellular distribution of YFP signal in both cells (Fig. 23). These results suggest that MTMR3/4 DKO cells exhibited accumulation of PtdIns3P.

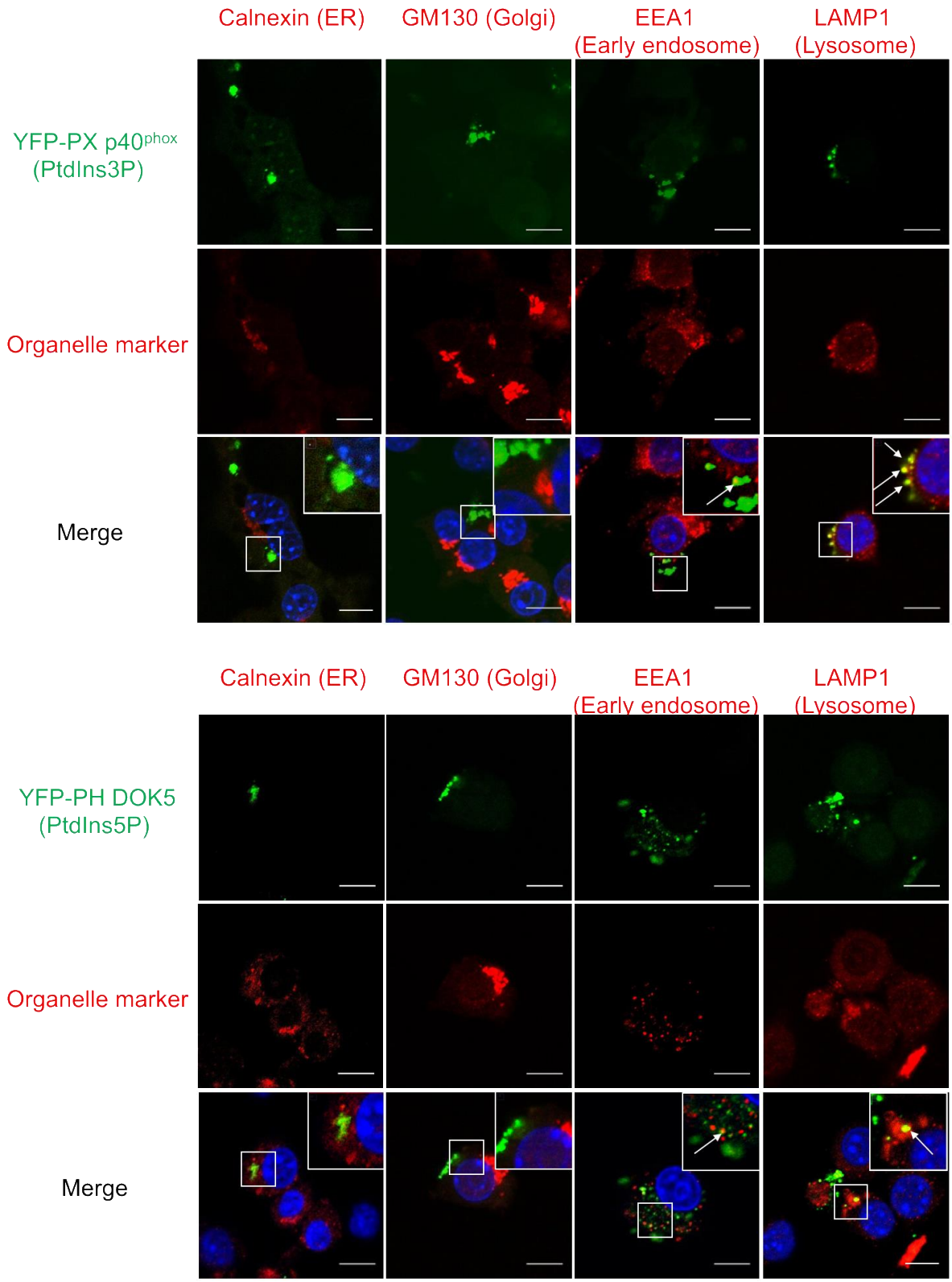

Fig. 22. Localization of PX p40^{phox} and PH DOK 5. RAW264.7 cells were expressed with YFP- PX-p40phox. (a) and YFP-PH-DOK 5 (b) and were stained with indicated antibodies; calnexin (endoplasmic reticulum), EEA (early endosome) and GM130 (Golgi), LAMP1 (Lysosome) (red). Scale bar 10 μm.

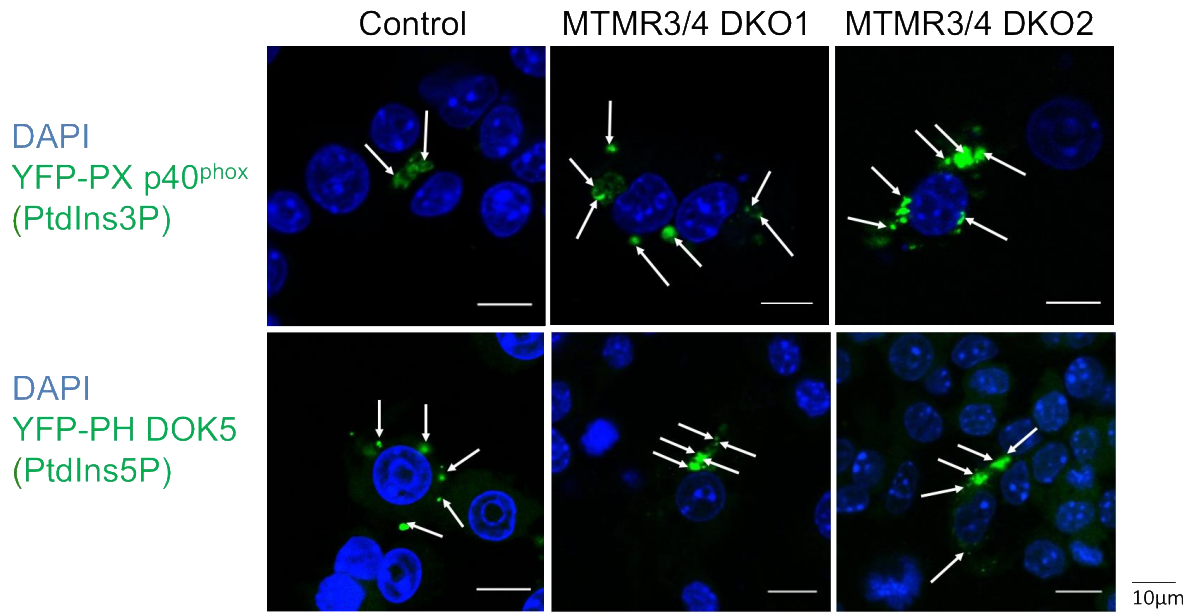

Fig. 23. Comparison of PX p40^{phox} and PH DOK5 localization in control and MTMR3/4 DKO cells. RAW264.7 cells were expressed with YFP-PX p40^{phox} and YFP-PH DOK5 in control and MTMR3/4 DKO cells. Scale bar 10 μm.

3.5 MTMR3/4 regulates STING trafficking from ER to Golgi

It has been shown that STING localized to ER in steady state and changes its localization to Golgi followed by the endosomes in response to DNA stimulation (Gonugunta et al., 2017). To visualize STING trafficking in MTMR3/4 DKO, I established control and MTMR3/4 DKO cells stably expressing FLAG-tagged STING using retrovirus transfer system, and co-stained them with anti-FLAG antibody and the endosome marker. The translocation of STING from ER to Golgi occurred within 1 and 4 hours after ISD stimulation in both control and MTMR3/4 DKO cells (Fig. 24). Interestingly, MTMR3/4 DKO cells showed STING translocation from ER to Golgi occurs within 1 hour after ISD stimulation whereas control cells did not show trafficking to Golgi at 1 hour, suggesting that STING trafficking from ER to Golgi is rapid in the absence of MTMR3 and MTMR4 and this is responsible for increased responses to DNA in DKO cells. These results also suggest that MTMR3/4 controls STING trafficking by regulating PtdIns3P production.

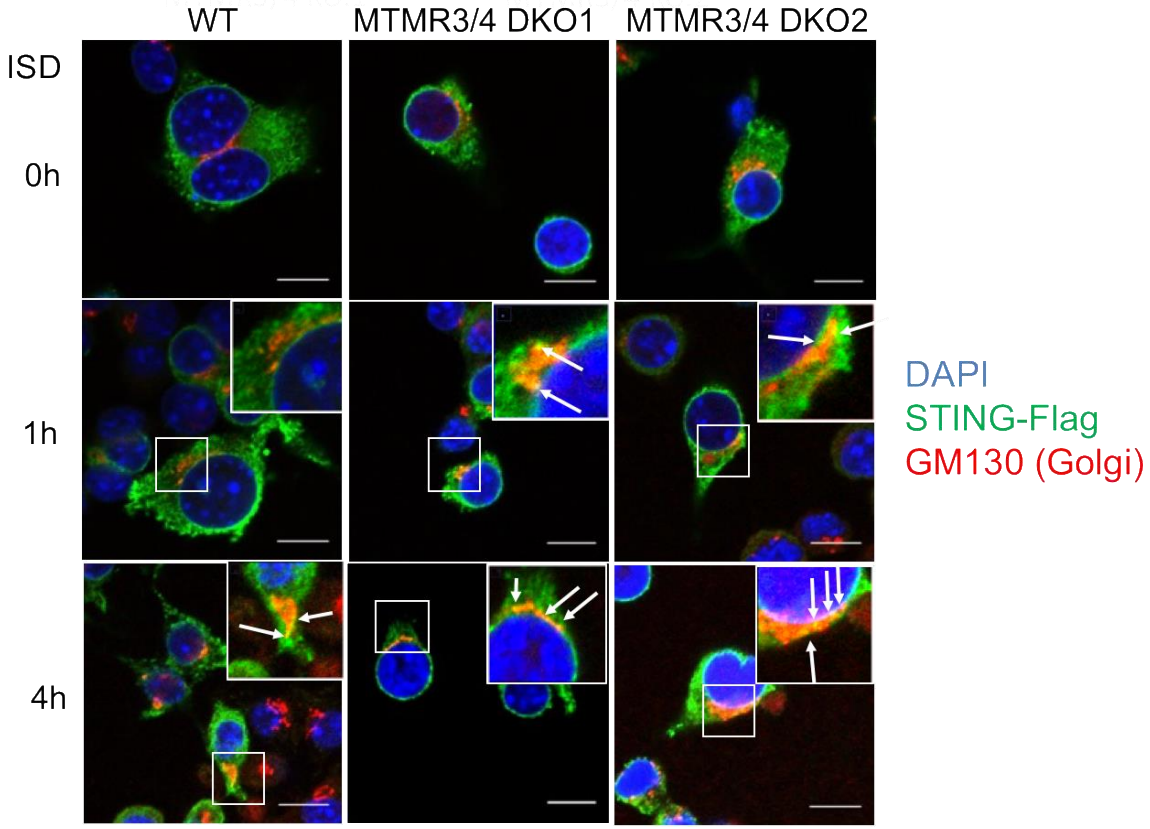

Fig. 24. Localization of STING. Control and MTMR3/4 DKO cells were expressed STING-Flag and were stimulated with and without ISD for 1hr and 4h. Scale bar 10 μm.

I next examined the localization of PX p40^{phox} and STING in control and MTMR3/4 DKO cells (Fig. 25). STING was co-localized with YFP-PX p40^{phox} in MTMR3/4 DKO cells after ISD 1h stimulation whereas STING was not co-localized in control cells. Co-localization of STING and PX-p40^{phox} was not observed without stimulation in control and MTMR3/4 DKO cells. In addition, triple staining with anti-EEA antibody showed that YFP-PX p40^{phox} positive puncta were located in early endosome in MTMR3/4 DKO cells, but not in control cells. These results suggest that accumulation of PtdIns3P by MTMR3/4 deficiency modulates trafficking of STING from ER to early endosome and Golgi.

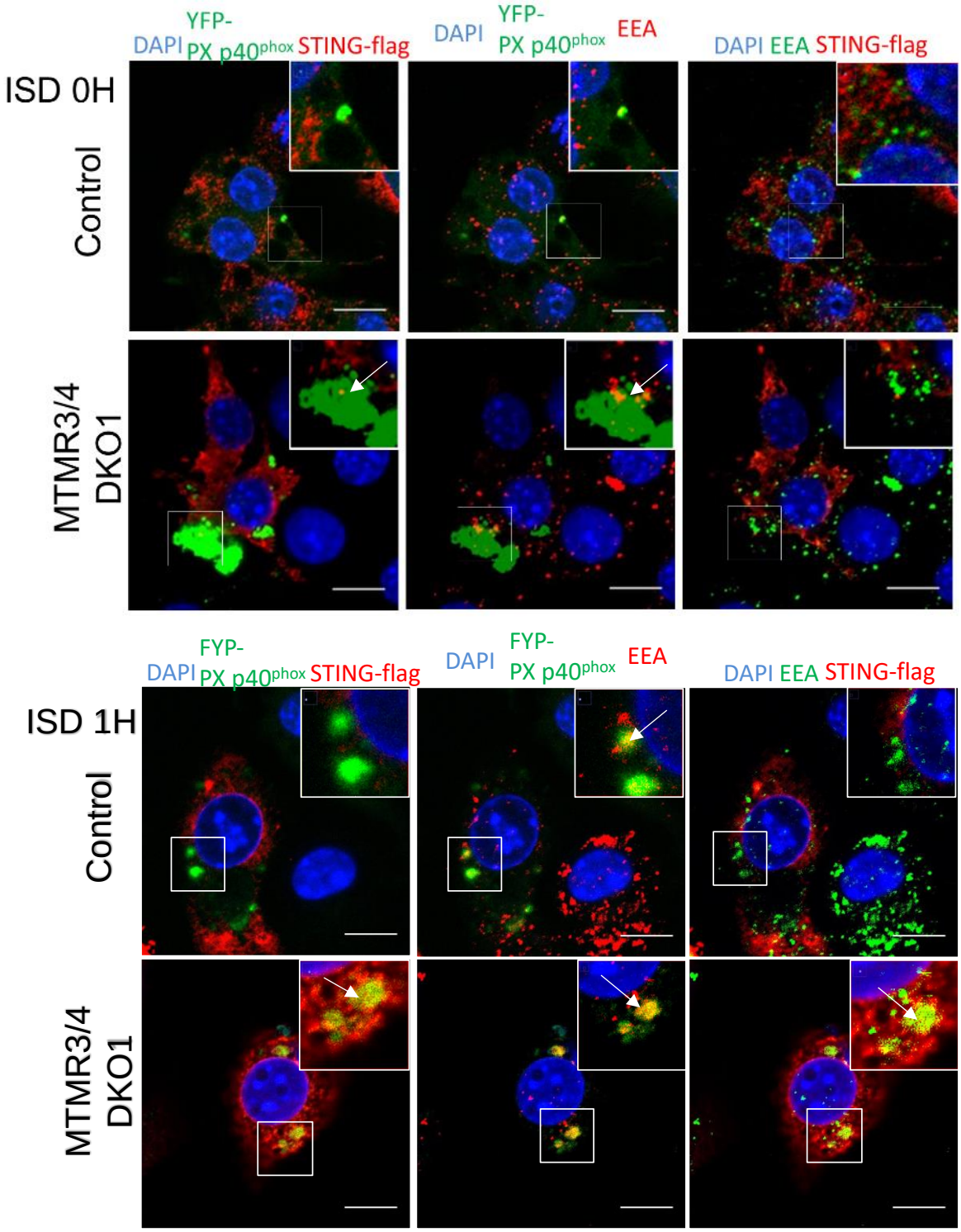

Fig. 25. STING and YFP-PX p40^{phox} localization. Control and MTMR3/4 DKO cells were expressed YFP-PX p40phox and STING-Flag and stimulated with ISD for 1h. Cells were stained with anti-Flag and anti-EEA (early endosome) antibody. Scale bar 10 μm.

4. Discussion

In this study, I revealed the functional role of MTMR3 and MTMR4 in innate immune response. I addressed expression of MTM family members and found that they are widely expressed in various types of cells including macrophages (Fig. 5). I also addressed their expression level after LPS, Poly I:C and ISD stimulation in RAW264.7 cells, but these stimulations did not dramatically change their expression (data not shown). Among the MTM family members, MTMR3 and MTMR4 belong to the same subfamily and have characteristic domain feature having FYVE domain and PH-Gram domain (Clague and Lorenzo, 2005). Therefore, I examined the role of MTMR3 and MTMR4 in innate immune responses. First, I performed IFNβ-promoter reporter assay but neither overexpression of MTMR3 nor MTMR4 drove the IFNβ promoter activation. However, overexpression of MTMR3 and MTMR4 together significantly inhibited the IFNβ promoter activity induced by STING overexpression. In contrast, IFNβ-promoter activity induced by IPS-1, MyD88 and TRIF overexpression was not inhibited by MTMR3 and MTMR4 co-expression (Fig. 8). Thus, MTMR3 and MTMR4 are suggested to specifically dampen STING-dependent IFNβ-promoter activating pathway.

To further investigate the role of MTMR3 and MTMR4 in macrophages, I generated MTMR3 and MTMR4-deficient RAW264.7 cells. The cytokine induction in single MTMR3 or MTMR4 KO cells following stimulation with ISD, Poly I:C and LPS were comparable with control cells (Fig. 10, Fig. 14). Moreover, phosphorylation of the transcription factor such as IRF3 and NF-κB was also comparable between control and KO cells. These results indicated that either MTMR3 or MTMR4 is not involved in innate immune responses to ISD, Poly I:C and LPS. However, it is notable that MTMR3/4 DKO cells showed significantly increased *Ifnb, Il6,* and *Cxcl10* expression following ISD stimulation. These cells also showed enhanced IRF3 phosphorylation after ISD stimulation (Fig. 13). These results were consistent with the results on the IFNβ promoter assay overexpressed with MTMR3/4. Thus, both MTMR3 and MTMR4 together may play important roles in the regulation of signal transduction in DNA sensing innate immune response.

MTMR3 and MTMR4 have abilities to dephosphorylate PtdIns3P and PtdIns3,5P_2 to generate PtdIns and PtdIns5P, respectively. MTMR3/4-deficiencies may thus induce PtdIns3P increment / PtdIns decrease, and/or PtdIns (3,5) P_2 increment / PtdIns5P decrease. Notably, DKO cells showed enlarged YFP-PX $p40^{phox}$ (binding to PtdIns3P) positive dot-like structure

compared to control cells, indicating accumulation of PtdIns3P in MTMR3/4 DKO cells. In contrast, signals in YFP-PH-DOK5 (binding to PtdIns5P)-expressing DKO cells did not show remarkable differences with those in YFP-PH-DOK5-expressing control cells, suggesting that production of PtdIns5P was not abrogated. Previous reports demonstrated that PtdIns5P production was decreased by inhibition of MTMR3 or MTMR4 activity (Oppelt et al., 2013) whereas PtdIns3P production was increased by MTMR4 knockdown or expression of inactive mutant for MTMR4 (MTMR4^{C407}) and MTMR3 knockdown (Naughtin et al., 2010; Lahiri et al., 2015). My results only supported that PtdIns3P production was increased by MTMR3/4-deficiencies, but not support PtdIns5P reduction. It is unclear why MTMR3/4-deficiencies in RAW264.7 did not affect PtdIns5P production. It is thought that PtdIns5P production in macrophages may be dominantly regulated by other enzymes such as PIKfyve since our laboratory previously demonstrated that PtdIns5P production in macrophages is decreased by PIKfyve knockdown. PIKfyve knockdown also impaired IRF3 phosphorylation after stimulation with RLR ligands (Kawasaki et al., 2013). Thus, PIKfyve may be responsible for PtdIns5P production even in the absence of MTMR3 and MTMR4 in macrophages.

STING localizes in the ER in a steady state and rapidly traffics to Golgi apparatus after stimulation with ISD (Shu et al., 2014; Chen et al., 2016; Gonugunta et al., 2017). I hypothesized that accumulation of PtdIns3P by MTMR3/4-deficiencies may change the STING translocation. My results showed that STING in both control and DKO cells reached to Golgi after 4h stimulation, but it is noted that STING in DKO cells translocated more rapidly to Golgi apparatus than control cells (Fig. 25). It is shown that TBK1 is recruited to STING-positive puncta after DNA stimulation, and becomes activated, suggesting that TBK1 translocation to Golgi apparatus and subsequent activation is coupled to IRF3 activation. Thus, rapid translocation of STING from ER to Golgi may contribute to enhanced innate immune responses in DKO cells by recruiting TBK1 to STING positive vesicles.

It was reported that PtdIns3P is mainly accumulated in early endosome, but it also widely spreads in other cellular endosomes (Friedman et al., 2013). Moreover, PtdIns3P is well-known to regulate autophagosome formation. Autophagy initiates its biogenesis through a pre-autophagosome double-membrane structure that is a subdomain of ER membrane positive for PtdIns3P and PtdIns3P-binding proteins (Axe et al., 2008). Consistently, it is reported that knockdown of MTMR3 increased autophagosome formation (Taguchi et al., 2010) while increased MTMR3 expression reduced autophagy (Lahiri et al., 2015). On the other hand, disruption of autophagy-related protein in mice is shown to result in increased inflammation and type I IFNs production during innate immune signaling pathways. My results showing that

PtdIns3P is increased in DKO cells suggest that autophagy formation is accumulated in these cells, and have a role in suppression of inflammation. However, our results showed DKO cells rather exhibited enhanced innate immune responses during STING activation. These results suggest that autophagosome formation has not participated in STING activation in DKO cells irrespective of increased PtdIns3P. Alternatively, a rapid translocation of STING to Golgi in DKO cells may negatively regulate PtdIns3P-dependent autophagosome formation via unknown pathways. The relationship between autophagy and MTMR3/4-dependent STING regulation should be understood in the future.

My results demonstrate that STING translocate from ER to Golgi at earlier time point in MTMR3/4 DKO cells than in control cells. This suggests that accumulation of PtdIsn3P by MTMR3/4-deficiencies enhances translocation of STING. ER has a dynamics and complex membrane network that extends to others endosomal organelle. Recent studies suggested that autophagosome biogenesis is initiated at a contact site of ER to other organelles, such as mitochondria and plasma membrane (Hamasaki et al., 2013; Zhuang et al., 2017), suggesting that PtdIns3P is generated at a specific site in ER. Because STING localizes to ER in the steady state, a functional interaction between STING and PtdIns3P in ER may be responsible for the trafficking of STING to Golgi. It is unclear how PtdIns3P regulates STING translocation, but several GPCR and ion channel are reported to bind to PtdIns (4,5) P_2 and regulate their functions. One possibility is that PtdIns3P may also directly bind to STING and induce the change of STING conformation, which induces translocation of STING to Golgi. Association of PtdIns3P with STING is really suggested by our observation (Fig. 25). Another possibility is that PtdIns3P provides a platform for association of STING and STING-regulatory proteins such as iRhom2, TRIM32 and TRIM56.

In this study, I found that MTMR3/4-deficiencies caused PtdIns3P accumulation, but did not cause PtdIns5P reduction. Accumulation of PtdIns3P was correlated with a rapid translocation of STING from ER to Golgi as well as enhanced IRF3 activation and type I IFN production. Although regulatory role of translocation of STING is still unclear, this study showed that PtdIns metabolism is important in fine turning innate immune responses to DNA. Self-DNA is aberrantly recognized by cGAS when it is released from the cytoplasm after host cells are died by necrosis or damaged by stresses, drugs and infection. This results in unwanted activation of STING pathway and appears to be highly associated with inflammatory and autoimmune diseases (Ahn and Barber, 2014; Li et al., 2017). Thus, MTMR3 and MTMR4 may be potential as a target of drug design that can prevent these diseases. Also, it is important to analyze a mutation or SNP in MTMR3 and MTMR4 genes in these diseases. Moreover, I

found aberrant formation of PtdIns3P positive puncta in MTMR3/4 DKO. This suggests that in disease conditions such as autoimmunity or in cells that are damaged or stressed, enlarged PtdIns3P positive puncta formation may be observed. Thus, it is also important to examine when these abnormal puncta formation is observed in some situations. This approach may lead to development of the strategy to predict onset of autoimmunity or inflammatory diseases.

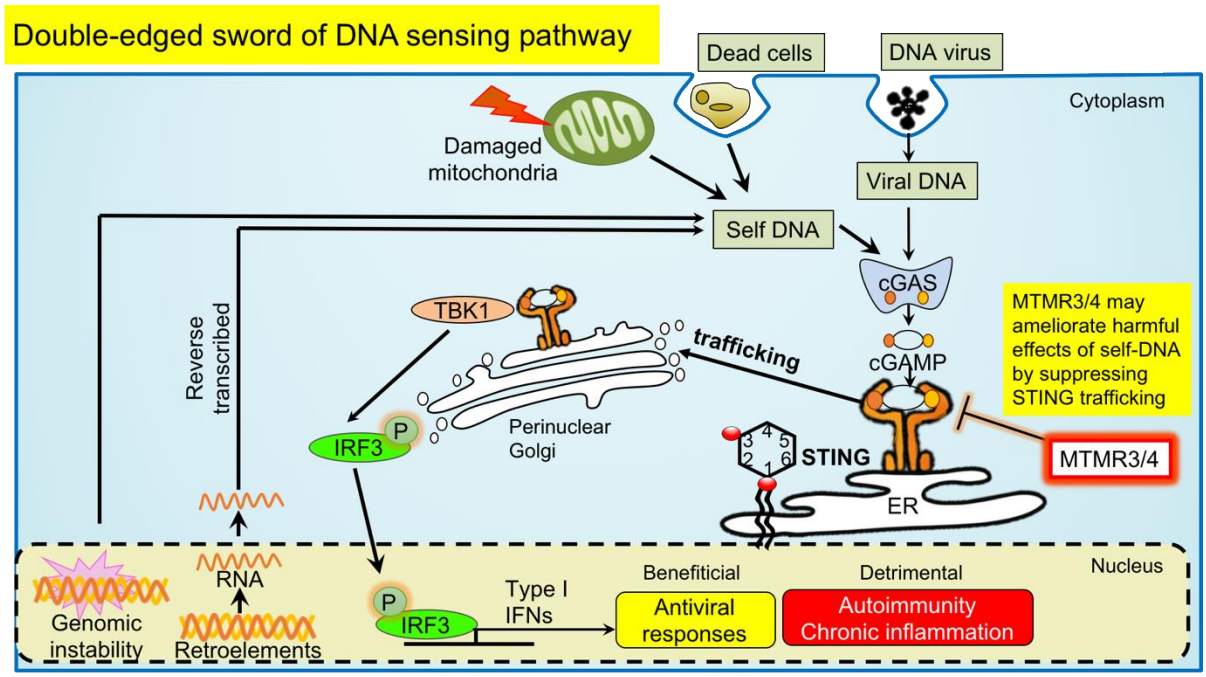

Fig. 26. Double-edge sword of DNA sensing pathway. Viral DNA can activate STING pathways that induce the antiviral response which is a beneficial for the host. Besides, self-DNA is often recognized by STING pathway when host cells are engulfed dead cells, mitochondria is damaged, genetic DNA is released into the cytoplasm as a result of genetic instability or reverse-transcription of retro−element. This aberrant recognition of self-DNA is detrimental because constitutive type I IFNs and inflammatory cytokines production leads to autoimmunity and chronic inflammatory diseases.

5. Acknowledgement

First, I would like to say الْحَمْدُ لِلَّهِ رَبِّ الْعَالَمِينَ (Alhamdulillahirabbil'aalamiin) to Al-Mighty Allah swt, the Most Merciful for always guide me to complete my research and for my beloved prophet messenger Muhammad saw.

My sincerely thank for my research supervisor, Prof. Taro Kawai, for advising my research and improving writing and supporting me throughout my doctoral course in NAIST. It is an honor for me to be one of his students in Lab. of Molecular Immunobiology, Graduate School of Biological Sciences, NAIST. I also deeply thank Dr. Takumi Kawasaki, who advised my research directions, supported me fully to conduct this research and improved my research skill. I send my gratitude to Dr. Daisuke Ori for his invaluable guidance and support for my research project. I would also like to offer my gratitude to NAIST scholarship for supporting me with a scholarship to study in NAIST. My appreciation also goes Dr. Motoya Murase, Masataka Kinoshita, Dr. Takuya Sueyoshi and Tomoya Deguchi for discussing and supporting my work. And I also appreciate for former and current members of Lab of Molecular Immunobiology who always supported me either in the lab or daily life, especially Mizuka Nagayama and Yusuke Harano. I thank the secretaries Kayo Abe and Chihiro Suzuki who helped me to conduct the administration. I give my gratitude to the staffs in international office of NAIST and office of Bioscience for their help regarding some administrative matters during my stay in Japan. I also deeply thank for Sachiko Iida for living place (apartment) support since I extended.

Finally, I send my deep gratitude to my family, mother, father and sisters for the huge support and sincerity that motivate me to always move forward.

6. References

Alexander, C., & Rietschel, E. T. (2001). Invited review: bacterial lipopolysaccharides and innate immunity. *Journal of endotoxin research*, *7*(3), 167-202.

Abe, T., & Barber, G. N. (2014). Cytosolic DNA-Mediated, STING-Dependent Pro-Inflammatory Gene Induction Necessitates canonical NF-κB activation Through TBK1. Journal of virology, JVI-00037

Ahn, J., & Barber, G. N. (2014). Self-DNA, STING-dependent signaling and the origins of autoinflammatory disease. *Current opinion in immunology*, *31*, 121-126.

Axe, E.L., Walker, S.A., Manifava, M., Chandra, P., Roderick, H.L., Habermann, A., Griffiths, G. and Ktistakis, N.T. (2008). Autophagosome formation from membrane compartments enriched in phosphatidylinositol 3-phosphate and dynamically connected to the endoplasmic reticulum. *The Journal of cell biology*, *182*(4), pp.685-701.

Barber, G. N. (2014). STING-dependent cytosolic DNA sensing pathways. Trends in immunology, 35(2), 88-93.

Bell, E. (2008). Innate immunity: TLR4 signalling. Nature Reviews Immunology, 8(4), 241.

Broz, P., & Monack, D. M. (2013). Newly described pattern recognition receptors team up against intracellular pathogens. *Nature Reviews Immunology*, *13*(8), 551.

Cai, X., Chiu, Y. H., & Chen, Z. J. (2014). The cGAS-cGAMP-STING pathway of cytosolic DNA sensing and signaling. Molecular cell, 54(2), 289-296.

Chen, Q., Sun, L., & Chen, Z. J. (2016). Regulation and function of the cGAS–STING pathway of cytosolic DNA sensing. Nature immunology, 17(10), 1142.

Chiang, J.J., Davis, M.E., and Gack, M.U. (2014). Regulation of RIG-I-like receptor signaling by host and viral proteins. Cytokine Growth Factor Rev. *25*, 491–505.

Clague, M. J., & Lorenzo, Ó. (2005). The myotubularin family of lipid phosphatases. *Traffic*, *6*(12), 1063-1069.

Costa, C., Martin-Conte, E.L., &Hirsch, E. (2011). Phosphoinositide 3-kinase p110 in immunity. *IUBMB life*, 63(9), 707-713.

Costa, C., Ebi, H., Martini, M., Beausoleil, S.A., Faber, A.C., Jakubik, C.T., Huang, A., Wang, Y., Nishtala, M., Hall, B. and Rikova, K. (2015). Measurement of PIP 3 levels reveals an unexpected role for p110β in early adaptive responses to p110α-specific inhibitors in luminal breast cancer. *Cancer cell*, *27*(1), pp.97-108.

Denis, N., Gupta, G. D., Lin, Z. Y., Gonzalez-Badillo, B., Pelletier, L., & Gingras, A. C. (2015). Myotubularin-related proteins 3 and 4 interact with polo-like kinase 1 and centrosomal protein of 55 kDa to ensure proper abscission. *Molecular & Cellular Proteomics*, *14*(4), 946-960.

Dobbs, N., Burnaevskiy, N., Chen, D., Gonugunta, V. K., Alto, N. M., & Yan, N. (2015). STING activation by translocation from the ER is associated with infection and autoinflammatory disease. *Cell host & microbe*, *18*(2), 157-168.

Ellson, C. D., & Yaffe, M. B. (2009). PX Domains. In Handbook of Cell Signaling (Second Edition) (pp. 1103-1109).

Favre, C., Gerard, A., Clauzier, E., Pontarotti, P., Olive, D., & Nunes, J. A. (2003). DOK4 and DOK5: new Dok-related genes expressed in human T cells. Genes and immunity, 4(1), 40.

Friedman, J. R., DiBenedetto, J. R., West, M., Rowland, A. A., & Voeltz, G. K. (2013). Endoplasmic reticulum–endosome contact increases as endosomes traffic and mature. Molecular biology of the cell, 24(7), 1030-1040.

Gonugunta, V. K., Sakai, T., Pokatayev, V., Yang, K., Wu, J., Dobbs, N., & Yan, N. (2017). Trafficking-Mediated STING Degradation Requires Sorting to Acidified Endolysosomes and Can Be Targeted to Enhance Anti-tumor Response. Cell reports, 21(11), 3234-3242.

Hamasaki, M., Furuta, N., Matsuda, A., Nezu, A., Yamamoto, A., Fujita, N., Oomori, H., Noda, T., Haraguchi, T., Hiraoka, Y. and Amano, A. (2013). Autophagosomes form at ER–mitochondria contact sites. *Nature*, *495*(7441), p.389.

Hnia, K., Vaccari, I., Bolino, A., & Laporte, J. (2012). Myotubularin phosphoinositide phosphatases: cellular functions and disease pathophysiology. Trends in molecular medicine, 18(6), 317-327.

Hu, M.M., Yang, Q., Xie, X.Q., Liao, C.Y., Lin, H., Liu, T.T., Yin, L. and Shu, H.B. (2016). Sumoylation promotes the stability of the DNA sensor cGAS and the adaptor STING to regulate the kinetics of response to DNA virus. Immunity, 45(3), pp.555-569.

Ishikawa, H., & Barber, G. N. (2008). STING is an endoplasmic reticulum adaptor that facilitates innate immune signalling. Nature, 455(7213), 674.

Irving, A., & Williams, B. R. (2009). Latest advances in innate antiviral defence. F1000 biologyreports, 1.

Kagan, J. C., Su, T., Horng, T., Chow, A., Akira, S., & Medzhitov, R. (2008). TRAM couples endocytosis of Toll-like receptor 4 to the induction of interferon-β. *Nature immunology*, *9*(4), 361.

Kanai, F., Liu, H., Field, S.J., Akbary, H., Matsuo, T., Brown, G.E., Cantley, L.C. and Yaffe, M.B., 2001. The PX domains of p47phox and p40phox bind to lipid products of PI (3) K. Nature cell biology, 3(7), p.675.

Kawai, T., and Akira, S. (2010). The role of pattern-recognition receptors in innate immunity: update on Toll-like receptors. Nat. Immunol. *11*, 373–384.

Kawai, T., Takahashi, K., Sato, S., Coban, C., Kumar, H., Kato, H., Ishii, K.J., Takeuchi, O., and Akira, S. (2005). IPS-1, an adaptor triggering RIG-I- and Mda5-mediated type I interferon induction. Nat. Immunol. *6*, 981–988.

Kawai, T., & Akira, S. (2011). Toll-like receptors and their crosstalk with other innate receptors in infection and immunity. *Immunity*, *34*(5), 637-650.

Kawasaki, T., Takemura, N., Standley, D. M., Akira, S., & Kawai, T. (2013). The second messenger phosphatidylinositol-5-phosphate facilitates antiviral innate immune signaling. *Cell host & microbe*, *14*(2), 148-158.

Konno, H., Konno, K., & Barber, G. N. (2013). Cyclic dinucleotides trigger ULK1 (ATG1) phosphorylation of STING to prevent sustained innate immune signaling. Cell, 155(3), 688-698.

Lahiri, A., Hedl, M., & Abraham, C. (2015). MTMR3 risk allele enhances innate receptor-induced signaling and cytokines by decreasing autophagy and increasing caspase-1 activation. *Proceedings of the National Academy of Sciences*, *112*(33), 10461-10466.

Lemmon, M. A. (2008). Membrane recognition by phospholipid-binding domains. Nature reviews Molecular cell biology, 9(2), 99.

Liu, S., Cai, X., Wu, J., Cong, Q., Chen, X., Li, T., Du, F., Ren, J., Wu, Y.T., Grishin, N.V. and Chen, Z.J. (2015). Phosphorylation of innate immune adaptor proteins MAVS, STING, and TRIF induces IRF3 activation. *Science*, *347*(6227), p.aaa2630.

Li, Y., Wilson, H. L., & Kiss-Toth, E. (2017). Regulating STING in health and disease. Journal of Inflammation, 14(1), 11.

Liu, X., & Wang, C. (2016). The emerging roles of the STING adaptor protein in immunity and diseases. Immunology, 147(3), 285-291.

Loo, Y. M., & Gale Jr, M. (2011). Immune signaling by RIG-I-like receptors. *Immunity*, *34*(5), 680-692.

Lorenzo, Ó., Urbé, S., & Clague, M. J. (2005). Analysis of phosphoinositide binding domain properties within the myotubularin-related protein MTMR3. Journal of cell science, 118(9).

Lau, L., Gray, E. E., Brunette, R. L., & Stetson, D. B. (2015). DNA tumor virus oncogenes antagonize the cGAS-STING DNA-sensing pathway. *Science*, *350*(6260), 568-571.

Luo, W. W., Li, S., Li, C., Lian, H., Yang, Q., Zhong, B., & Shu, H. B. (2016). iRhom2 is essential for innate immunity to DNA viruses by mediating trafficking and stability of the adaptor STING. Nature immunology, 17(9), 1057.

Ma, Z., & Damania, B. (2016). The cGAS-STING defense pathway and its counteraction by viruses. *Cell host & microbe*, *19*(2), 150-158.

Seo, G. J., Kim, C., Shin, W. J., Sklan, E. H., Eoh, H., & Jung, J. U. (2018). TRIM56-mediated monoubiquitination of cGAS for cytosolic DNA sensing. Nature communications, 9(1), 613.

Shim, H., Wu, C., Ramsamooj, S., Bosch, K.N., Chen, Z., Emerling, B.M., Yun, J., Liu, H., Choo-Wing, R., Yang, Z. and Wulf, G.M. (2016). Deletion of the gene Pip4k2c, a novel phosphatidylinositol kinase, results in hyperactivation of the immune system. *Proceedings of the National Academy of Sciences*, *113*(27), pp.7596-7601.

Tronchère, H., Laporte, J., Pendaries, C., Chaussade, C., Liaubet, L., Pirola, L., ... & Payrastre, B. (2004). Production of phosphatidylinositol 5-phosphate by the phosphoinositide 3-phosphatase myotubularin in mammalian cells. Journal of Biological Chemistry, 279(8), 7304-7312.

Mackenzie, K.J., Carroll, P., Martin, C.A., Murina, O., Fluteau, A., Simpson, D.J., Olova, N., Sutcliffe, H., Rainger, J.K., Leitch, A. and Osborn, R.T., 2017. cGAS surveillance of micronuclei links genome instability to innate immunity. Nature, 548(7668), p.461.

Naughtin, M.J., Sheffield, D.A., Rahman, P., Hughes, W.E., Gurung, R., Stow, J.L., Nandurkar, H.H.,Dyson, J.M. and Mitchell, C.A., (2010). The myotubularin phosphatase MTMR4 regulates sorting from early endosomes. Journal of cell science, pp.jcs-060103.

Oppelt, A., Lobert, V.H., Haglund, K., Mackey, A.M., Rameh, L.E., Liestøl, K., Schink, K.O., Pedersen, N.M., Wenzel, E.M., Haugsten, E.M. and Brech, A., (2013). Production of phosphatidylinositol 5-phosphate via PIKfyve and MTMR3 regulates cell migration. *EMBO reports*, *14*(1), pp.57-64.

Oppelt, A., Haugsten, E.M., Zech, T., Danielsen, H.E., Sveen, A., Lobert, V.H., Skotheim, R.I. and Wesche, J., (2014). PIKfyve, MTMR3 and their product PtdIns5P regulate cancer

cell migration and invasion through activation of Rac1. Biochemical Journal, 461(3), pp.383-390.

Pandey, S., Kawai, T., & Akira, S. (2014). Microbial sensing by Toll-like receptors and intracellular nucleic acid sensors. Cold Spring Harbor perspectives in biology, a016246.

Saitoh, T., Fujita, N., Hayashi, T., Takahara, K., Satoh, T., Lee, H., Matsunaga, K., Kageyama, S., Omori, H., Noda, T. and Yamamoto, N., (2009). Atg9a controls dsDNA-driven dynamic translocation of STING and the innate immune response. Proceedings of the National Academy of Sciences, 106(49), pp.20842-20846.

Seth, R.B., Sun, L., Ea, C. K., and Chen, Z.J. (2005). Identification and characterization of MAVS, a mitochondrial antiviral signaling protein that activates NF-kappaB and IRF 3. Cell *122*, 669–682.

Shu, H. B., & Wang, Y. Y. (2014). Adding to the STING. Immunity, 41(6), 871-873.

Sun, L., Wu, J., Du, F., Chen, X., & Chen, Z. J. (2013). Cyclic GMP-AMP synthase is a cytosolic DNA sensor that activates the type I interferon pathway. Science, 339(6121), 786-791.

Srivastava, S., Li, Z., Lin, L., Liu, G., Ko, K., Coetzee, W. A., & Skolnik, E. Y. (2005). The phosphatidylinositol 3-phosphate phosphatase myotubularin-related protein 6 (MTMR6) is a negative regulator of the Ca2+-activated K+ channel KCa3. 1. *Molecular and Cellular Biology*, *25*(9), 3630-3638.

Taguchi-Atarashi, N., Hamasaki, M., Matsunaga, K., Omori, H., Ktistakis, N. T., Yoshimori, T., & Noda, T. (2010). Modulation of local PtdIns3P levels by the PI phosphatase MTMR3 regulates constitutive autophagy. Traffic, 11(4), 468-478.

Tsuchida, T., Zou, J., Saitoh, T., Kumar, H., Abe, T., Matsuura, Y., Kawai, T. and Akira, S., (2010). The ubiquitin ligase TRIM56 regulates innate immune responses to intracellular double-stranded DNA. Immunity, 33(5), pp.765-776.

Tronchère, H., Bolino, A., Laporte, J., & Payrastre, B. (2012). Myotubularins and associated neuromuscular diseases. *Clinical Lipidology*, *7*(2), 151-162.

Teo, W. X., Kerr, M. C., & Teasdale, R. D. (2016). MTMR4 is required for the stability of the Salmonella-containing vacuole. *Frontiers in cellular and infection microbiology*, *6*, 91.

Tooze, S.A., Jefferies, H.B., Kalie, E., Longatti, A., Mcalpine, F.E., Mcknight, N.C., Orsi, A., Polson, H.E., Razi, M., Robinson, D.J. and Webber, J.L., (2010). Trafficking and signaling in mammalian autophagy. *IUBMB life*, *62*(7), pp.503-508.

Wang, Q., Liu, X., Cui, Y., Tang, Y., Chen, W., Li, S., Yu, H., Pan, Y. and Wang, C., (2014). The E3 ubiquitin ligase AMFR and INSIG1 bridge the activation of TBK1 kinase by modifying the adaptor STING. *Immunity*, *41*(6), pp.919-933.

Wang, H., Hu, S., Chen, X., Shi, H., Chen, C., Sun, L., & Chen, Z. J. (2017). cGAS is essential for the antitumor effect of immune checkpoint blockade. Proceedings of the National Academy of Sciences, 201621363.

Wymann, M. P., & Schneiter, R. (2008). Lipid signalling in disease. *Nature reviews Molecular cell biology*, *9*(2), 162.

Xiong, M., Wang, S., Wang, Y. Y., & Ran, Y. (2018). The Regulation of cGAS. *Virologica Sinica*, 1-8.

Yang, H., Wang, H., Ren, J., Chen, Q., & Chen, Z. J. (2017). cGAS is essential for cellular senescence. Proceedings of the National Academy of Sciences, 114(23), E4612-E4620.

Yu, J., Pan, L., Qin, X., Chen, H., Xu, Y., Chen, Y., & Tang, H. (2010). MTMR4 attenuates TGFβ signaling by dephosphorylating R-Smads in endosomes. Journal of biological chemistry, jbc-M109.

Zou, J., Zhang, C., Marjanovic, J., Kisseleva, M. V., Majerus, P. W., & Wilson, M. P. (2012). Myotubularin-related protein (MTMR) 9 determines the enzymatic activity, substrate specificity, and role in autophagy of MTMR8. *Proceedings of the National Academy of Sciences*, *109*(24), 9539-9544.

Zhang, X., Shi, H., Wu, J., Zhang, X., Sun, L., Chen, C., & Chen, Z. J. (2013). Cyclic GMP-AMP containing mixed phosphodiester linkages is an endogenous high-affinity ligand for STING. Molecular cell, 51(2), 226-235.

Zhuang, X., Chung, K. P., Cui, Y., Lin, W., Gao, C., Kang, B. H., & Jiang, L. (2017). ATG9 regulates autophagosome progression from the endoplasmic reticulum in Arabidopsis. *Proceedings of the National Academy of Sciences*, *114*(3), E426-E435.